

ROQUIN Regulates *Cis*-Acting Elements within a Target mRNA

Xin Hu

March 2007

A thesis submitted for the Master of Philosophy degree of the
Australian National University



ROQUIN Regulates Cis-Acting
Elements within a Target mRNA

Xin Hu

March 2007

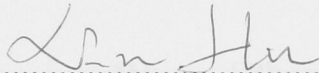
A thesis submitted for the Master of Philosophy degree of the
Australian National University



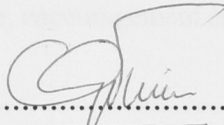
THE AUSTRALIAN NATIONAL UNIVERSITY

Statement of originality

The results presented in this thesis are, except where otherwise acknowledged, my own original work



Xin Hu



Supervisor: Carola Vinuesa

Acknowledgments

Carola

Above all, I wish to thank my supervisor Dr. Carola Vinuesa. Your wealth of knowledge and extraordinary ability never ceases to amaze me. These two years you have continuously provided generous academic, technical and emotional support. Carola is a brilliant scientist and mentor and I sincerely wish to thank you for the opportunity to study in the group. It has been an honour to learn from such a gifted researcher.

Di Yu

I am very grateful to my best friend Di Yu for your invaluable advice and encouragement and understanding throughout these two years. Thank you for your constant support, inexhaustible enthusiasm and your genuine eagerness to reach me a multitude of methods. Our friendship over the past two years has been unforgettable.

Diego Silva

Thank you for not only sharing your technical and academic expertise with me, but also for your care, encouragement and advice.

Robert Rigby, Connie Angelucci,

Thank you for the wealth of knowledge and support made available to me

IGL

Thank you for all your support throughout these years. IGL is the best group.

My Father and Grandmother

Thank you for your love
Grandmother's love can mend anything
Grandmother's love will live long past her years

Florina Lo

Thank you for your encouragement and understanding.

Abstract

Roquin is a recently identified autoimmune regulator. Mice with a loss of function mutation in *Roquin* have dysregulated Inducible Co-Stimulator (ICOS) expression on T cells and develop lupus and autoimmune diabetes. *Roquin*'s localization to stress granules and a CCCH zinc finger domain predicted to bind RNA suggest a role in post-transcriptional regulation of gene expression. Here, we investigate the molecular mechanisms by which *Roquin* suppresses ICOS expression. We have developed an experimental system that can accurately quantify the suppressive effect of *Roquin* on ICOS. Using this system, we have found the 3' untranslated region (3'UTR) of *Icos* contains *cis*-acting element(s) that mediates *Roquin*'s suppression. Fine mapping the 3'UTR has led to the identification of a small regulatory region responsible for *Icos* mRNA degradation. Software-based motif prediction within this small region has shed light into the molecular mechanisms by which *Roquin* exerts this regulation. We are also investigating the presence of similar *cis*-acting elements within the mRNAs of *Roquin*'s potential targets other than ICOS, such as TNF alpha.

Acknowledgement of other people's contribution to my work

- (1) The author's contribution to Chapter 3 was 60%. Di Yu performed the initial experiments using HEK 293T system and guided me in the implementation of the NIH3T3 system. His specific contribution has been acknowledged in the relevant chapter.
- (2) The author's contribution to Chapter 4 was 80%. Di Yu helped where indicated in the figure legends.
- (3) The author's contribution to Chapter 5 was 100%.

Therefore, the author's contribution was 80%.

List of Abbreviations

APC: Antigen Presenting Cell
ARE: AU-Rich Element
BCR: B Cell Receptor
CTLA-4: Cytotoxic T lymphocyte Antigen - 4
DC: Dendritic Cell
GC: Germinal Centre
DMEM: Dulbecco's Modified Eagle's Medium
GFP: Green Fluorescent Protein
HI-FBS: Heat Inactivated Fetal Bovine Serum
ICOS: Inducible Co-Stimulator
ICOSL: Inducible Co-Stimulator Ligand
IL: Interleukin
IFN: Interferon
IRES: Internal Ribosomal Entry Site
Ig: Immunoglobulin
LTR: Long Terminal Repeat
MFI: Mean Fluorescence Intensity
MHC: Major Histocompatibility Complex
MiRNA: MicroRNA
MSCV: Murine Stem Cell Virus
NO: Nitric Oxide
PBs: Processing Bodies
PMA: Phorbol Myristate Acetate
PSG: PIPES Salt Glucose
SGs: Stress Granules
SLE: Systemic Lupus Erythematosus
TCR: T Cell Receptor
TFH: T Follicular Helper Cell

TNF α : Tumor Necrosis Factor Alpha

Tia-1: T cell-induced antigen

TLR: Toll-Like Receptors

TTP: Tristetraprolin

T_H: T helper

UTR: Untranslated region

1	1.1	The spatial organization of mammalian genomes
2	1.2	Transcription factors
3	1.3	TGF β
4	1.3.1	TGF β
5	1.3.2	TGF β
6	1.3.3	TGF β
7	1.3.4	TGF β
8	1.4	The core cell cycle machinery
9	1.5	Chromatin remodeling and its regulation
10	1.6	Regulation of chromatin structure
11	1.7	The function of DNA 4-cisplatin
12	1.8	The DNA code
13	1.9	The K ₂ MEK2M pathway
14	1.10	MAPK signaling in development
15	1.11	The novel nuclear transcription factor
16	1.12	The structure of Kaposin protein
17	1.12.1	Structure and function of Kaposin protein
18	1.12.2	RNAi type zinc finger motif
19	1.12.3	C/EBP β zinc finger motif
20	1.12.4	The novel and highly conserved K ₂ domain
21	1.4	The regulation of K ₂ MEK2M
22	1.4.1	Transcriptional regulation
23	1.4.2	Post-transcriptional regulation
Chapter 2: Mammals and humans		
24	2.1	Neurological DNA methylation
25	2.2	Protein

Table of Contents

Chapter 1: General discussion

2	1.1	B cell differentiation during immune responses
2	1.1.1	The germinal center is a specialized microenvironment
2	1.1.2	T helper subsets
3	1.1.2.1	T _H 1 cells
3	1.1.2.2	T _H 2 cells
3	1.1.2.3	T _{FH} cells
4	1.1.2.4	T _H 17 cells
4	1.1.3	T _{FH} cells and autoimmunity
4	1.2	Costimulation: signaling and its regulation
4	1.2.1	Families of co-stimulatory signals
5	1.2.2	The CD28/CTLA 4 family
6	1.2.3	The <i>Icos</i> gene
6	1.2.4	The ICOS/ICOSL pathway
7	1.2.5	ICOS signaling in autoimmunity
7	1.3	The novel immune regulator Roquin
8	1.3.1	The structure of Roquin protein
8	1.3.1.1	Structure and function of Zinc finger motif
8	1.3.1.2	RING type zinc finger motif
9	1.3.1.3	CCCH Zinc finger motif
9	1.3.1.4	The novel and highly conserved ROQ domain
10	1.4	The regulation of ICOS expression
10	1.4.1	Transcriptional regulation
10	1.4.2	Post-transcriptional regulation

Chapter 2: Materials and methods

13	2.1	Recombinant DNA techniques
13	2.1.1	Vectors

13	2.1.1.1	Vector information
14	2.1.1.2	Preparing pR-IRES-huCD4 retroviral vector for <i>Icos</i> cDNA subcloning
14	2.1.2	<i>Icos</i> cDNA fragment
14	2.1.2.1	PCR amplification of <i>Icos</i> from cDNA template
17	2.1.2.2	Restriction enzyme digestion
17	2.1.2.3	Purification of DNA fragments
17	2.1.3	Generation of new retroviral constructs expressing different <i>Icos</i> cDNA fragments
17	2.1.3.1	Insertion of <i>Icos</i> cDNA fragments into pR-IRES-huCD4 retroviral vector
18	2.1.3.2	Chemical transformation of competent cells
18	2.1.3.3	Mini preparation of plasmid DNA (mini-prep)
18	2.1.3.4	Large scale preparation of plasmid DNA (maxi-prep)
19	2.1.3.5	Quantitation of DNA
19	2.1.3.6	DNA sequencing
20	2.2	New retrovirus constructs
20	2.2.1	Cell culture
21	2.2.2	Package retrovirus
21	2.2.3	Retroviral transduction
21	2.3	RNA extraction
22	2.4	cDNA synthesis
23	2.5	Real-time PCR
23	2.6	Flow cytometry
24	2.6.1	Antibodies used for flow cytometry
24	2.7	Common buffers and chemicals
24	2.7.1	Phosphate buffer saline (PBS)
24	2.7.2	Tris-acetate-EDTA (TAE) electrophoresis buffer
24	2.7.3	EtBr staining buffer
25	2.7.4	FACS wash buffer
25	2.7.5	Agarose gel loading dye
25	2.7.7	5x sequencing buffer

25	2.7.7	Ampicillin agar culture plate
25	2.7.8	Hepes buffered saline (HBS) buffer
26	2.8	Statistic analysis
26	2.9	Bioinformactics tools

Chapter 3: *Icos* 3'UTR is required to mediate Roquin's repression

28	3.1	Introduction
35	3.2	Development of a retrovirus-mediated transduction system to investigate the regulation of target mRNA by Roquin
38	3.3	The 3'UTR, but not the coding region within <i>Icos</i> mRNA is required for Roquin's regulation
47	3.4	Summary

Chapter 4: The distal fragment within *Icos* 3'UTR contains the cis-acting element(s) and promotes Roquin's mediated *Icos* mRNA decay

51	4.1	Introduction
54	4.2	F3 within 3'UTR is required for the repression of ICOS by Roquin
57	4.3	F3 within 3'UTR is sufficient for the repression of ICOS by Roquin
61	4.4	F3 within <i>Icos</i> mRNA 3'UTR mediates Roquin's promotion of mRNA degradation
64	4.5	Summary

Chapter 5: TNF alpha is also a target for post-transcriptional regulation by Roquin

67	5.1	Introduction
70	5.2	Roquin regulates TNF α expression through its 3'UTR
73	5.3	Roquin ^{M199R} increases transcripts encoding <i>Tnf</i> α 3'UTR
76	5.4	Roquin ^{M199R} increases transcripts in a gene-dose dependent manner
76	5.5	The 3'UTR of <i>Tnf</i> α mRNA contains AREs and microRNA target sequences
78	5.6	Summary

Chapter 6: General discussion

- 80 6.1 Limiting ICOS expression emerges as a novel mechanism to maintain immune tolerance
- 82 6.2 The role of ROquin in promoting *Icos* mRNA decay
- 83 6.3 The M199R mutation in Roquin impairs but does not abolish ICOS repression
- 83 6.4 How does Roquin regulate mRNA decay
- 85 6.5 A potential role for microRNAs in the regulation of *Icos* mRNA
- 85 6.6 TNF alpha and other putative targets of Roquin's regulation
- 87 6.7 Model

Chapter 7: References

§ ONE §

General introduction

1.1 B cell differentiation during immune responses

B cells secrete antibody that plays multiple protective roles in the face of infection. Antibodies neutralize viruses and toxins, opsonise extracellular bacteria, activate complement, and activate other cells including natural killer cells. B cell activation by protein antigens requires both binding of the antigen by B cell surface Ig: the B-cell receptor and interaction of the B cell with a primed antigen-specific helper T cell. This first cognate T: B cell interaction usually occurs in the T zones of secondary lymphoid tissues. After receiving T cell help, B cells differentiate along one of two pathways:

- (1) In the extrafollicular pathway B cells give rise to short lived unmutated plasma cells.
- (2) In the follicular pathway, B cells enter follicles and give rise to germinal centres (GCs)

1.1.1 The Germinal center is a specialized microenvironment

T-dependent humoral immune responses are characterized by the development of GCs in B cell follicles of the secondary lymphoid organs. Within these structures, B cells undergo somatic hypermutation targeted at the Immunoglobulin (Ig) variable (V) region genes. These mutations change the affinity of the B cell. While the goal is the production of high affinity mutants, loss of antigen reactivity and acquisition of self-reactive specificities can also occur (Diamond and Scharff, 1984; Winkler *et al.*, 1992). Importantly, the germinal center environment filters the repertoire of differentiating B cells such that high affinity variants are preferentially selected while low affinity or self-reactive clones are eliminated by apoptosis (Hoch *et al.*, 2000; Shokat and Goodnow, 1995; Smith *et al.*, 2000; Takahashi *et al.*, 1999). Follicular B helper T cells (T_{FH}) are responsible for supporting Ig production and probably selecting high affinity mutants (Liu *et al.*, 1989). Selected cells can then go on to differentiate into either memory B cells or long-lived plasma cells, which generally home to the bone marrow.

1.1.2 T helper subsets

The differentiation of CD4 T cells into T helper subsets determines whether humoral or cell-mediated immunity will predominate, and regulates B cell differentiation, selection, and activation of other effector cell types including macrophages. All T helper subsets express the CD4 co-receptor and recognize fragments of antigens degraded within intracellular vesicles, displayed at the cell surface by MHC class II molecules.

There are at least four subsets of CD4⁺ helper cells: Th1, Th2, Th17, T_{FH}; and at least three of them (Th1, Th2, T_{FH}) can provide help to B cells (Harrington et al., 2005; Mosmann and Sad, 1996; Vinuesa et al., 2005b):

1.1.2.1 T_h1 cells:

These cells control infection with intracellular pathogens, including viruses and bacteria (Sher and Reis e Sousa, 1998; Thierfelder et al., 1996). T_h1 cell differentiation requires IL-12 secretion by antigen-presenting cells (APCs) and the T cell transcription factors T-bet, STAT4 and STAT1 (Szabo et al., 2000). T_h1 cells secrete IFN- γ and tumor necrosis factor (TNF), and induce mouse B cell switching towards IgG2a (Cher and Mosmann, 1987; Stevens et al., 1998) T_h1 cells have been thought to mediate many autoimmune diseases although a number of them now appear to be mediated by T_h17 cells instead (Furuzawa-Carballeda et al., 2007; Weaver et al., 2006)

1.1.2.2 T_h2 cells:

T_h2 cells control infection with helminths and other extracellular microbes and are, in part, the effectors that mediate the immunopathology of allergic responses and asthma (Janeway et al., 2004). Th2 cell differentiation requires the cytokine IL-4 produced during T cell priming by APCs (and mast cells), and the T cell transcription factors STAT6 and GATA3 (Ansel et al., 2006; Kaplan et al., 1996; Zheng and Flavell, 1997). T_h2 cells secrete IL-4, IL-5, and IL-13, and induce B cell switching predominantly to IgG1 (in mice) (Mosmann and Coffman, 1989; Stevens et al., 1988).

1.1.2.3 T_{FH} cells:

T_{FH} cells localize to the follicles and typically express the highest levels of ICOS and the chemokine receptor CXCR5, which binds CXC-chemokine ligand 13 (CXCL13) that is a chemokine that is secreted by follicular stromal cells and T_{FH} cells themselves (Breitfeld et al., 2000; Hutloff et al., 1999; Kim et al., 2001; Schaerli et al., 2000). They are specialized in providing help to germinal center B cells during antibody responses to T cell-dependent antigens (reviewed in (Vinuesa et al., 2005)). They also express the transcription factor Bcl-6 and B cell co-stimulatory molecules including CD40L and IL-21 (Chtanova et al., 2004).

1.1.2.4. T_h17 cells:

T_H17 cells appear to protect against fungal antigens, secrete IL-17 (both IL-17A and IL-17F) and expand in response to IL-23 independently of T-bet or STAT1 but dependent on STAT3 (Acosta-Rodriguez et al., 2007; Harris et al., 2007; Yang et al., 2007). In mice, polarization of naïve $CD4^+$ T cells toward the T_H17 lineage requires a combination of T cell antigen receptor (TCR) stimulation, the cytokines TGF- β , IL-6 and IL-21 (Korn et al., 2007; Nurieva et al., 2007; Zhou et al., 2007), and expression of the transcription factor ROR γ t (Ivanov et al., 2006). T_H17 cells have been shown to mediate organ-specific autoimmune diseases including experimental allergic encephalomyelitis, collagen-induced arthritis, and inflammatory bowel disease (Langrish et al., 2005; Park et al., 2005; Weaver et al., 2007)

1.1.3 T_{FH} cells and autoimmunity

Immunity is controlled by checks and balances. Evidence from a number of studies indicates that self-antigens are abundant in germinal centers. In particular nuclear antigens are known to be exposed on the surface of apoptotic cells in the form of membrane blebs (Casciola-Rosen et al., 1994).

Since B cells undergo somatic hypermutation within germinal centres that can potentially give rise to the emergence of self-reactive B cells, tolerance check-points must be in place to eliminate B cells with self reactive specificities. In principle this can be achieved by preventing activated self-reactive T cells entering follicles and providing help to self-reactive germinal center B cells (Vinuesa et al., 2005). In this way, self-reactive germinal center B cells will be precluded from differentiation to become plasma cells and memory cells (Goodnow et al., 2005). There are two mechanisms that have been described that curtail self-reactive T_{FH} from providing aberrant help to self-reactive B cells. The first mechanism depends on $CD4^+CD25^+CD69^-$ regulatory T cells (Tregs) (Lim et al., 2004). In the second mechanism, the Roquin pathway appears to repress accumulation of self-reactive T cells within germinal centers (Vinuesa et al., 2005a).

1.2 Co-stimulation: signaling and its regulation

1.2.1 Families of co-stimulatory signals

Importantly, naïve T cells require two signals for full activation (Janeway et al., 2004).

The first is antigen-specific and based on recognition of peptide/ MHC complexes by the T cell receptor (TCR). The second signal is an antigen non-specific co-stimulatory signal, delivered by molecules expressed on the surface of antigen presenting cells (APCs).

T cell activation and function is regulated by the innate and adaptive immune systems, through positive and negative co-stimulatory signals (Greenwald et al., 2005). The best described co-stimulatory molecules belong to the B7 superfamily. B7 ligands are expressed by APCs (dendritic cells, B cells and macrophages) and play key roles in regulating T cell activation and tolerance (Sharpe and Freeman, 2002). Manipulation of co-stimulation has promising therapeutic value in a number of autoimmune and inflammatory conditions. These pathways not only provide critical positive second signals that promote and sustain T cell responses, but they also contribute critical negative second signals, such as through CTLA-4 and PD-1 that down-regulate T cell activation (Carreno and Collins, 2002). These negative signals function to limit, terminate, and/or attenuate T cell responses, and they appear to be especially important for regulating T cell tolerance and autoimmunity (Abbas et al., 2004).

1.2.2 The CD28/CTLA 4 family

The CD28 family of co-stimulatory molecules expanded with the discovery of T cell Inducible Co-Stimulator (ICOS) in 1999 by Kroczeck and colleagues (Hutloff et al., 1999). In this super family, ICOS, CD28, cytotoxic T lymphocyte antigen 4 (CTLA-4), and programmed cell death protein (PD-1) share several structural and functional similarities (Sharpe and Freeman, 2002). The B7-CD28/CTLA-4 co-stimulatory pathway is the best characterized T cell co-stimulatory pathway and is complex because of the dual specificity of B7-1(CD80) and B7-2(CD86) for the stimulatory receptor CD28 and inhibitory receptor CTLA-4 (CD152) (Greenwald et al., 2005). CD28 delivers signals important for T cell activation and survival; in contrast CTLA-4 inhibits T cell responses and regulates peripheral T cell tolerance (Burmeister et al., 2008; Greenwald et al., 2005). ICOS is inducibly expressed on T cells upon priming, and plays important roles in the development and/or effector function of, Th1, Th2, T_{FH} cells, CD8⁺ cytotoxic T cells and Treg cells (Akbari et al., 2002; Greenwald et al., 2005; Hutloff et al., 1999; Burmeister et al., 2008).

CD28/B7; ICOS/ICOSL and CD40L/CD40 interactions are known to be necessary for T

cell-dependent antibody production, isotype switching, and germinal center formation (Sharpe and Freeman, 2002). Humans and mice deficient for any of these ligand/receptor pairs exhibit absent or impaired germinal center formation, B cell memory production and production of switched antibody. While defects in CD40/CD40L and B7/CD28 signaling affect earlier stages in the immune response including T cell priming, the effects of ICOS deficiency or deficiency of its ligand are more confined to the impairment of germinal centre responses (Dong et al., 2001a; Dong et al., 2001b; Mak et al., 2003; McAdam et al., 2001; Tafuri et al., 2001; Wong et al., 2003)

1.2.3 The *Icos* gene

In humans, *Icos* is located on chromosome 2q33 in a tight cluster with CD28, CTLA4, and PD-1. Interestingly, this region has been associated with both autoimmune and hypersensitivity diseases such as multiple sclerosis, systemic lupus erythematosus (SLE), and asthma, all of them are associated with potentially pathogenic antibody responses (Coyle and Gutierrez-Ramos, 2004; Graham et al., 2006).

ICOS consists of five exons with 2620 nucleotides (NM_012092) coding for a 199 amino acid protein. The 5 prime untranslated region (5'UTR) of ICOS is 35 nucleotides in length and the coding region is 600 nucleotides long (from 36 to 635 bps). The 3'UTR is 1895 nucleotides long (from 636 to 2620 bps).

1.2.4 The ICOS/ICOSL pathway

As mentioned above, the ICOS: ICOSL pathway appears to be particularly important for stimulating effector T cell responses and T cell-dependent B cell responses. In naïve T cells that do not express ICOS, ICOS is upregulated upon T cell priming (Hutloff et al., 1999). The highest levels of ICOS are found on T_{FH} cells, in fact ICOS^{high} expression is one of the most reliable phenotypic features of this subset (Vinuesa et al., 2005). All other effector CD4⁺ cells besides T_{FH} cells also express ICOS, albeit lower levels (Yoshinaga et al., 1999). Expression of ICOS by Tregs has been suggested to be important for their suppressor function (Akbari et al., 2002). Although ICOS levels persist at higher levels on T_h1 cells than they do on T_h2 cells (Greenwald et al., 2005), there is evidence to suggest ICOS expression is more critical for T_h2 function rather than for T_h1 (Hutloff et al., 1999).

In a manner similar to CD28, ICOS signaling augments T cell activation during effector responses and cytokine production. In the absence of CD28, ICOS can compensate and allow sufficient co-stimulation for immune responses to take place (Suh et al., 2004). As mentioned above, ICOS-ICOS-L interactions also provide critical signals for B cell differentiation into memory cells within germinal centers and maintain TFH cell longevity (Akiba et al., 2005).

Mice deficient in ICOS have poor T-dependent antibody responses with impaired germinal centre formation, and very low numbers of switched and memory B cells (Dong et al., 2001b; McAdam et al., 2001; Tafuri et al., 2001). Humans with mutations in ICOS suffer from common variable immunodeficiency (CVID) and lack memory B cells (Grimbacher et al., 2003). Thus, ICOS signaling guarantees the longevity of humoral immune responses.

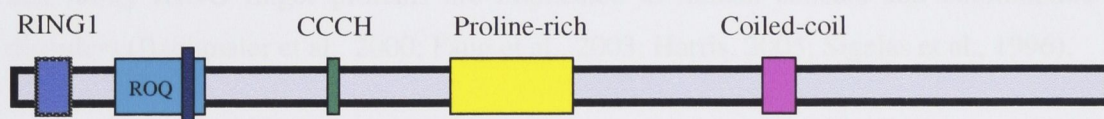
1.2.5 ICOS signaling in autoimmunity

While ICOS deficiency leads to T and B cell immunodeficiency (Grimbacher et al., 2003), several studies suggest that dysregulated ICOS signaling may lead to autoimmunity. Blockade of ICOS-ICOS-L interactions have been shown to ameliorate autoantibody-mediated autoimmune disease in mice (i.e. collagen-induced arthritis, experimental allergic encephalomyelitis and lupus-like syndromes) (Iwai et al., 2003; Iwai et al., 2002; Rottman et al., 2001). Overexpression of ICOS-L using an ICOS-L-Fc transgenic led to hypergammaglobulinemia (Yoshinaga et al., 1999), although there was no report of autoimmunity in these mice. Human patients with lupus and rheumatoid arthritis have been reported to express high levels of ICOS on their T cells (Hutloff et al., 2004; Kawamoto et al., 2006; Okamoto et al., 2003; Yang et al., 2005), but until now it has been unclear whether this is a cause or an effect. More recently, *sanroque* mice, carrying a mutant form of Roquin (Roquin^{M199R}) have been shown to overexpress ICOS in a T cell autonomous fashion, and develop systemic autoimmunity (lupus) and organ-specific autoimmunity (autoimmune diabetes). During the course of this work, our laboratory has established that Roquin^{M199R}-induced ICOS overexpression is directly responsible for the lymphadenopathy, splenomegaly, and T and B cell accumulation found in *sanroque* mice (Yu et al., 2007). In summary, ICOS appears to play an important role in the maintenance of self-tolerance, and thus understanding its regulation is potentially important for the improved diagnosis and treatment of several autoimmune diseases.

1.3 The novel immune regulator Roquin

The *Roquin* gene was identified during a search for novel autoimmune regulators in the mouse genome (Vinuesa et al., 2005a; Vinuesa and Goodnow, 2004). As mentioned above, *sanroque* mice homozygous for a mutant allele of Roquin (*san*; M199R) develop lupus-like disease. The human *Roquin/Rc3h1* gene can be found on chromosome 1 within the 1q25 locus. Roquin consists of 20 exons. The transcript length is 4,094 bps and the translated product is 1,133 residues. The Roquin protein is highly conserved across species. It contains an amino-terminal RING-1 zinc-finger at residues 14-53 that conforms perfectly to the consensus for the E3 ubiquitin ligase family of proteins. From residues 131 to 360, there is a novel protein domain named ROQ domain, which harbours the M199R mutation found in *sanroque* mice. A zinc-finger motif of the C-X₈-C-X₅-C-X₃-H type (CCCH type zinc finger) occurs distal to the ROQ domain, from residues 419-438 (Vinuesa et al., 2005a). Roquin also contains a large proline-rich region, predicted to contain multiple binding sites for SH3 domain-containing proteins, and two coiled-coil domains that may mediate dimerisation of this protein.

1.3.1 The structure of Roquin protein



(Vinuesa et al., 2005a)

1.3.1.1 Structure and function of Zinc finger motifs

The name “zinc finger” was coined based on a two-dimensional diagram of a typical domain structure resembling a finger and these proteins have multiple copies of folded domains that contain conserved cysteines and histidines binding to zinc. The zinc-finger motif is an important group of DNA-binding motifs with one or more zinc atoms as structure components. There are several different types and combinations of Cys-Cys (CC) or Cys-His (CH) motifs that comprise the zinc finger family, which is found in over 100 transcription factors, E3 ubiquitin ligases, and RNA-regulating proteins. I will briefly describe the two zinc fingers that are found in Roquin.

1.3.1.2 RING type zinc finger motif

The first report of a RING finger motif was published in 1991 by Freemont and colleagues. Initially, the motif was identified by searching sequence databases and using the N-terminal sequence of a gene named RING1 (really interesting new gene 1). Within the past twenty years, the three-dimensional structure and biological function of the RING finger motif has become apparent.

The RING finger motif is a C_3HC_4 zinc-finger motif and can be defined as $C-X_2-C-X_{(10-45)}-C-X_1-C-X_7-H-X_2-C-X_{(11-25)}-C-X_2-D$ (Koken et al., 1995). Roquin's RING motif conforms perfectly to the consensus for the E3 ubiquitin ligase family of proteins (Pfam00642), which includes Lnx, Traf 4, Rbx and Cbl. Roquin's RING finger motif has recently been shown to have an ubiquitin ligase activity: the *C.elegans* homologue of Roquin, RLE-1, mediates ubiquitylation of DAF-16 via its RING finger motif (Li et al., 2007).

Ubiquitination generally targets proteins for degradation in the proteasome, although it can also mediate recycling of membrane-bound proteins and direct them to lysosomal compartments. RING finger proteins such as MDM2, c-Cbl, or BRCA1, have been shown to play a critical role in degradation of regulatory proteins. Some of these proteins regulate cellular proteins that prevent tumorigenesis. Some reports have shown that faulty RING finger proteins are implicated in human cancers and autoimmune disorders (Bachmaier et al., 2000; Fang et al., 2003; Harris, 2005; Sigalas et al., 1996).

1.3.1.3 CCCH Zinc finger motif

In recent years, some studies identified that Cys-Cys-Cys-His (CCCH)-containing proteins are involved in the post-transcriptional control of gene expression. CCCH zinc finger motifs can bind to RNA and destabilize it (or in less frequent cases, stabilize it) via AU-Rich-Elements (ARE) present in the target RNA sequence (Carballo *et al.*, 1998; Carrick *et al.*, 2004). Roquin's CCCH motif is shared by tristetraprolin (TTP), Pos-1, CPSF30K/Yth1p, TbZP1 and TcZFP1 (Carballo *et al.*, 1998; Carrick *et al.*, 2004; Taylor *et al.*, 1996). Recent evidence suggests the CCCH motif can help the accelerate mRNA degradation by enhancing the mRNA decay process initiated after removal of the polyadenylated (polyA) tail from mRNA. In this way, TTP mediates ARE-dependent *Tnf* mRNA degradation (Blackshear, 2002). RNA-binding proteins

containing CCCH-Zinc fingers can also regulate post-transcriptional regulation of gene expression at the level of translation.

1.3.1.4 The novel and highly conserved ROQ Domain

The novel protein Roquin contains an extraordinarily conserved novel domain, named ROQ domain (Vinuesa et al., 2005a). This domain appears to be critical for Roquin's localization to stress granules and for the induction of stress granule formation upon Roquin overexpression (Athanasopoulos V, personal communication). It is in this domain where Roquin's ^{M199R} mutation responsible for the lupus phenotype of *sanroque* mice lies.

1.4 The regulation of ICOS expression

1.4.1 Transcriptional regulation

The critical role of ICOS in co-stimulating T cell responses is well documented. As its name indicates ICOS is induced during T cell activation. However, there is not much knowledge about the mechanisms that regulate ICOS expression. A recent study using signal pathway-specific inhibitors has shown that the transcription of *Icos* was enhanced by the signals through Fyn-calcineurin-NFATc2 and MEK2-ERK1/2 pathway (Tan et al., 2006).

1.4.2 Post-transcriptional regulation

Although there is as yet no evidence that ICOS expression is regulated post-transcriptionally, the localization of Roquin to SGs, a hub of mRNA decay and translational inhibition, and its putative RNA binding CCCH domain suggests the possibility of post-transcriptional regulation of ICOS.

Recent studies have highlighted the critical role of the regulation of mRNA turnover to enable cells including T lymphocytes, to rapidly respond to environment stimuli by changing the amounts of critical mRNAs encoding cytokines and chemokines (Cheadle et al., 2005; Fan et al., 2002). The rapid decay of mRNA is determined by specific *cis*-acting elements. Among them, AU-rich elements (AREs) have been found and functionally characterized (Brooks *et al.*, 2004). As mentioned above, TTP can regulate mRNA stability of *Tnf* via its 3'UTR containing AREs (Blackshear, 2002; Carballo *et*

al., 1998).

Besides AREs, other cis-acting elements that regulate mRNA translation and stability, such as microRNA (miRNA), have also been identified. The first miRNA, *lin-4*, was found in 1993 (Lee *et al.*, 1993). MiRNAs have attracted attention as a new class of small non-coding RNAs regulating the expression of genes that are involved in various biological processes, such as development, cell proliferation, and apoptosis (Kloosterman and Plasterk, 2006; Lee *et al.*, 2004; Wienholds and Plasterk, 2005). MiRNAs have been shown to bind miRNA target sequences within the 3'UTR of target mRNAs and mediate post-transcriptional repression of gene expression (Jackson and Standart, 2007). The number of known miRNAs in mammals has risen dramatically, and their total number in humans has been predicted to be as high as 1,000 (Berezikov and Plasterk, 2005; Chang and Mendell, 2007).

§ TWO §

Materials and methods

pR-IRES5-huCD4

Multiple cloning site (MCS) sequence

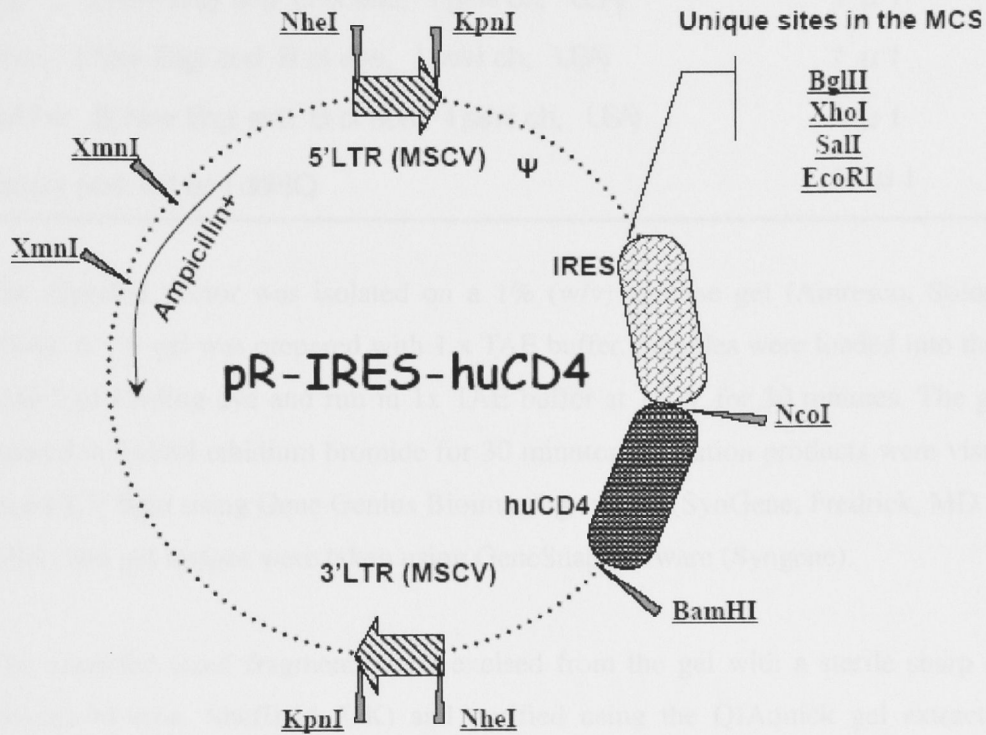
5'-GGG...GAC-3'
ATG TCTG CAGGCTG GACGGTATCGATAAGC
3'-TCAATATC GATTC GCGGCGCGGCGCTAAGC
5'-TCACTGGGCTGAGGCGGCTTGGATATGAGGCGC
GGTGTGCGC

2.1 Recombinant DNA techniques

2.1.1 Vectors

2.1.1.1 Vector information

The schematic map of pR-IRES-huCD4 retroviral vectors is shown below.



Multiple cloning site (MCS) sequence

```

Bgl II   Xho I   Sal I
AGATCTCTCGAGGTCGACGGTATCGATAAGC
      EcoR I
TTGATATCGAATTCCGCCCCCCCCCCTAACG
TTACTGGCCGAAGCCGCTTGAATAAGGCC
GGTGTGCG
  
```

2.1.1.2 Preparing pR-IRES-huCD4 retroviral vector for *Icos* cDNA subcloning

pR-IRES hCD4 retroviral vector (1 µg) was digested for 3 hours at 37°C with the restriction enzymes Bgl II (1 µl) and Xho I(1 µl) in a 20µl reaction mix.

pR-IRES-huCD4 vector (0.5 µg/µl)	2 µl
Bgl II (New England Biolabs, Ipswich, USA)	1 µl
XhoI (New England Biolabs, Ipswich, USA)	1 µl
Buffer 2 (New England Biolabs, Ipswich, USA)	2 µl
Deionised water (ddH ₂ O)	14 µl

The digested vector was isolated on a 1% (w/v) agarose gel (Amresco, Solon, OH, USA). A 1% gel was prepared with 1 x TAE buffer. Samples were loaded into the wells with 5 µl loading dye and run in 1x TAE buffer at 150V for 30 minutes. The gel was stained in 1µl/ml ethidium bromide for 30 minutes. Digestion products were visualized under UV light using Gene Genius Bioimaging system (SynGene, Fredrick, MD 21704, USA) and gel images were taken using GeneSnap software (Syngene).

The expected sized fragments were excised from the gel with a sterile sharp scalpel (Swann-Morton, Sheffield, UK) and purified using the QIAquick gel extraction kit (QIAGEN, VIC, Australia). The gel slices were solubilized by incubating in buffer QG at 50°C for 10 minutes, and then they were applied to the column and centrifuged at 13,000 rpm for 1 minute in a microcentrifuge (Sigma Quantum Scientific). The column was washed with PE buffer by centrifuging at 13,000 rpm for 1 minute. Then the DNA was eluted by adding 20µl elution buffer to the column and centrifuging at 13,000 rpm for 1 minute.

2.1.2 *Icos* cDNA fragments

2.1.2.1 PCR amplification of *Icos* from cDNA template

The oligonucleotide primers used to amplify *Icos* cDNA fragments and expected product sizes are listed below. The sequences are denoted 5' to 3'.

Coding sequence (CDS)

Forward primer AAA AGA TCT TTC TGG CAA ACA TGA AG TCA G

Reverse primer

AAA CTC GAG CCA GAG TTC CAT ATT ATA GGG TCA

Product size

624 bps

Full length (FL)

Forward primer AAA AGA TCT CTG AAC GCG AGG ACT GGT A

Reverse primer

AAA CTC GAG TCA AAT GGT TAT TCT TTG CCT TCT T

Product size

2596 bps

Full length lacking F2 and F3 (Δ F2+F3)

Forward primer AAA AGA TCT CTG AAC GCG AGG ACT GGT A

Reverse primer

AAA CTC GAG AAA ACT ATT GAG CAG CAG AGG A

Product size

1348 bps

Full length lacking F3 (Δ F3)

Forward primer AAA AGA TCT CTG AAC GCG AGG ACT GGT A

Reverse primer AAA CTC GAG CTG TGA TTCCAGGGTGA

Product size

1884 bps

F1 of 3' UTR (3' UTR-F1)

Forward primer AAA AGA TCT TGA CCC TAT AAT ATG GAA CTC TGG

Reverse primer AAA CTC GAG AAA ACT ATT GAG CAG CAG AGG A

Product size 724 bps

F2 of 3' UTR (3' UTR-F2)

Forward primer AAA AGA TCT TCC TCT GCT GCT CAA TAG TTTT

Reverse primer

Reverse primer AAA CTC GAG CTG TGA TTCCCAGGGTGA

Product size

Product size 558 bps

F3 of 3' UTR (3' UTR-F3)

Forward primer AAA AGA TCT CTC CCA GAG GCT GAA GTC AC

Reverse primer

Reverse primer AAA CTC GAG TCA AAT GTT TAT TCT TTG CCT TCT T

Product size

Product size 763 bps

PCR reaction mix:

10 x <i>Pfu</i> buffer (<i>Stratagene</i>)	5 μ l
dNTPs (10mM dATP, dCTP, dGTP and dTTP)	1 μ l
Forward <i>O</i> igonucleotide primer (10 μ M <i>Gene works</i>)	1 μ l
Reverse <i>O</i> igonucleotide primer (10 μ M <i>Gene works</i>)	1 μ l
DNA template (10 ng/ μ l)	1 μ l
<i>Pfu</i> DNA polymerase (<i>Stratagene</i>)	1 μ l
Deionised water (ddH ₂ O)	40 μ l

PCR thermal program:

Step	Temperature	Duration	Cycle
Pre-denature	94 \square	120 (sec)	1
Denature	94 \square	30 (sec)	30
Annealing	60 \square	30 (sec)	
Elongation	68 \square	60 (sec) / kb	
After-elongation	68 \square	300 (sec)	1

2.1.2.2 Restriction enzyme digestion of PCR products

PCR products were separated on a 1% (w/v) agarose gel. The bands with expected size were excised from the agarose gel and purified using QIAquick gel extraction kit.

The gel purified fragments were restriction digested for 3 hours at 37°C with *Bgl* II (1 μ l) and *Xho*I (1 μ l):

Purified PCR product (<i>Icos</i> cDNA fragments)	5 μ l
<i>Bgl</i> \square (<i>New England Biolabs, Ipswich, USA</i>)	1 μ l
<i>Xho</i> \square (<i>New England Biolabs, Ipswich, USA</i>)	1 μ l
Buffer 2 (<i>New England Biolabs, Ipswich, USA</i>)	2 μ l
Deionised water (ddH ₂ O)	11 μ l

2.1.2.3 Purification of DNA fragments

After the reaction was performed the digestion production was run via electrophoresis on a 1%(w/v) agarose gel. The bands with expected size were excised from the agarose gel and purified using QIAquick gel extraction kit.

2.1.3 Generation of new retroviral constructs expressing different *Icos* cDNA fragments

2.1.3.1 Insertion of *Icos* cDNA fragments into pR-IRES-huCD4 retroviral vector

A ligation reaction was performed to insert Bgl-II-Xho-I digested *Icos* cDNA fragments into Bgl-II and Xho-I digested pR-IRES-huCD4 vector.

Bgl II and Xho I - digested pR-IRES-huCD4 vector (700µg)	3 µl
Bgl II and Xho I - digested <i>Icos</i> cDNA fragments (800µg)	14 µl
T4 DNA ligation buffer (Roche diagnose)	2 µl
T4 DNA ligase (Roche diagnose)	1 µl

The ligation reaction mix was incubated overnight at 16°C

2.1.3.2 Chemical transformation of competent cells

DH5α *E.coli* competent cells were heat-shocked in the presence of ligated products. The 20µl ligation reaction mix and 100µL DH5α competent cells (homemade) were incubated together on ice for 20 minutes and then shocked by incubation at 42°C for 60 seconds, followed by incubation on ice for 15 minutes. 250µl LB broth was added to the tube and incubated at 37°C with rigorous shaking for 45 minutes. The cells were spread on an ampicillin agar plate which would only permit growth of ampicillin-resistant cells, which is cells, containing the pR-IRES-huCD4 vector, which carry the ampicillin resistance gene. The agar plates were incubated overnight at 37°C.

2.1.3.3 Mini preparation of plasmid DNA (mini-prep)

Individual colonies were then selected and cultured overnight in LB broth with

ampicillin (100µg/ml). Plasmids were isolated from the cultures using QIAprep kit (QIAGEN, VIC, Australia) as per the manufacturer's instructions. Cultured cells were pelleted by centrifugation at 4000 rpm for 1 minute; the cells were resuspended in 250µl P1 buffer and transferred to a 1.5ml Eppendorf tube (Hamburg, Germany). Buffer P2, 250µl, was added and the tube mixed by inversion. 350µl of buffer N3 was added and the tube was mixed by inversion. The cellular debris was pelleted by centrifugation at 13,000 rpm for 10 minutes in a microcentrifuge (Sigma Quantum Scientific). The supernatant was applied to a QIAprep column and centrifuged for 1 minute at 13,000 rpm. The column was washed with 0.7 ml of buffer PB by centrifugation at 13,000 rpm for 1 minute. The DNA was then eluted with 50µL elution buffer by centrifuging for 1 minute at 13,000 rpm.

2.1.3.4 Large scale preparation of plasmid DNA (maxi-prep)

Plasmids were isolated from the cultures using Hurricane Maxi Prep Kit (GerardBiotech, US) as per the manufacturer's instructions. The culture was shaken at 250 RPM over night at 37°C until cell density was no more than $OD_{595} < 1.3$ and transferred to a 250ml centrifuge (Sorvall) tube. After centrifugation for 10 minutes at 5,000 x g at room temperature, the bacterial pellet was resuspended in 10 ml of Buffer A by pipetting. The resuspension was transferred to a 50 ml disposable centrifuge tube and 10 ml of Buffer B added. The suspension was mixed by inverting the tube 10 times and allowed to stand at room temperature for 5 min. To this, 13 ml of Buffer C was added and mixed by inversion 10 times. The mixture was transferred to a high speed centrifuge tube and centrifuged for 10 min. at 14,000 - 18,000 x g at 4 °C. The supernatant was carefully transferred to a 50 ml disposable centrifuge tube and kept at 4 °C. The supernatant was added to the DNA Binding Column Unit and centrifuged for 5 min. at 5,000 x g at 4 °C to bind the DNA. After discarding the liquid from the collection tube, the remaining supernatant was added to the column and re-centrifuged. The excess liquid was discarded and the DNA bound to the column was washed with 20 ml of 70% ethanol and centrifuged at 5,000 x g for 5 minutes at 4 °C. The ethanol wash was repeated. Any excess ethanol was removed from the centrifuge tube by centrifugation (10 min, 5,000 xg, RT) and air drying the column for 10 min. The DNA binding column was carefully transferred into a new 50 ml collection tube. To elute the DNA from the column, 1ml of heated ddH₂O was added to the column and left at RT for 1 min. The column was centrifuged for 5 min at 5000xg at RT. Plasmids were stored at -20°C.

2.1.3.5 Quantitation of DNA

The preparation of plasmid DNA was quantified using NanoDrop. The concentrations of DNA samples from maxi-preps usually range from 500ug/ul to 1500ug/ul; the concentrations of DNA samples from mini-preps usually range from 200ug/ul to 400ug/ul.

2.1.3.6 DNA sequencing

The oligonucleotide primers used to sequence *HuICOS* FL constructs are listed below. The sequences are denoted 5' to 3'.

Forward primer	CTCCACAATGGACGGATTTC
Reverse primer	ACTCCAGAAGCAATGCCTGT

Sequencing PCR reaction mix:

5 x sequencing buffer (BioMolecular Resource Facility, JCSMR ANU)	4 μ l
Forward Oligonucleotide primer (10 μ M Gene works)	2 μ l
DNA template (10 ng/ μ l)	5 μ l
Big dye terminator (BioMolecular Resource Facility, JCSMR ANU)	1 μ l
Deionised water (ddH ₂ O)	6 μ l

After preparing the reaction mixture, each sample was performed in a 200 μ l thin-walled 96-well plate (Quality Scientific Plastics) using a MJ Research PTC-225 Peltier Thermal cycler.

PCR thermal program:

Step	Temperature	Duration	Cycle
Pre-denaturation	96° C	300 (sec)	1
Denaturation	96° C	30 (sec)	30
Annealing	50° C	15 (sec)	
Elongation	60° C	90 (sec)	
After-elongation	60° C	240(sec)	1

The sequencing products were precipitated for submission. The samples were transferred to a 1.5ml tube and 1µl EDTA (50mM), 50µl absolute EtOH and 1µl NaOAc (1.5M) were added. After centrifugation at 13000 rpm for 30 minutes at room temperature, the supernatant was removed carefully. The pellet was washed with 250µl 70% ethanol and centrifuged at 13000 rpm for 15 minutes at room temperature. The supernatant was removed and pellet washed again. Then, the DNA pellet was dried by centrifugation under vacuum and submitted for sequencing.

2.2 New retrovirus constructs

2.2.1 Cell culture

Phoenix cell line

The Phoenix cell line is derived from HEK293T cell line and is used for retroviral packaging. This cell line was cultured in complete Dulbecco's Modified Eagles Medium (DMEM) (SAFC, Bioscience, USA) supplemented with 2% PSG and 10% HI-FCS and at 37°C, with 5% CO₂.

NIH 3T3 cell line

The NIH 3T3 cell line is a mouse embryonic fibroblast cell line. This cell line was cultured in complete DMEM (SAFC, Bioscience, USA) supplemented with 2% PSG and 10% HI-FCS and at 37°C, with 5% CO₂.

2.2.2 Packaging of retroviruses

The retroviruses expressing either Roquin, *Icos* cDNA fragments or empty vector were

packaged in Phoenix cells by transfecting Phoenix cells with individual constructs. One day before transfection, Phoenix cells growing in culture were split and added 4×10^6 cells into a new 160ml tissue culture flask (Nunc, Roskilde, Denmark) and the cells incubated overnight at 37°C in 20ml DMEM (JRH biosciences, VIC, Australia) until they were 70-80 % confluent. The culture medium was replaced after 30-40 minutes with 10ml DMEM with 25nM chloroquine and incubated at 37°C . For the transfection, 2500 μl transfection mix (1250 μl 2 x HBS buffer, 25-30 μg of the plasmid diluted in 1000 μl sterile H_2O and 250 μl calcium chloride (1.25 M)) was added drop-wise to the phoenix cell culture flask and cells were incubated at 37°C . Fresh DMEM was added 6 hours after transfection to replace the transfection media. The cells were incubated for 24 hours at 37°C , and then at 30°C for another 24 hours. The culture supernatant containing retroviral particles was harvested and stored at -80°C .

2.2.3 Retroviral transduction

NIH3T3 cells were cultured at 2×10^6 per ml in DMEM (SAFC, Bioscience. USA) for 24 hours, and then spin-co-transduced with retroviral supernatant containing 40 ul/ml polybrene (Sigma, Germany) in six wells plates (NUNC, Denmark) at 30°C and 2500rpm for 90 minutes. After 2 hours the media in each well with transduction reagents was replaced with fresh media, and then incubated in 37°C for another 48 hours.

2.3 RNA extraction

Cell pellets are stored at -70°C in Trizol (Invetrogen, USA). All RNA work is done in a specified RNA room under sterile conditions. This involved taking precautions to avoid RNA degradation by Rnases. After allowing the Trizol samples to thaw out, they are left for 10 minutes at room temperature. 0.2 ml of Chloroform per 1ml of Trizol is added to each tube and tubes are shaken vigorously for 15 seconds. The samples are then incubated at room temperature for 2-3 minutes and then centrifuged at 14,000 rpm at 4°C for 10 minutes. After spinning three separate layers should be visible, the eppendorf tube is held against a light source to clearly see three different layers. The top layer is Chloroform, containing RNA; the middle layer contains debris of proteins and DNA while the bottom layer is Trizol. The top layer containing the RNA is carefully aspirated, trying not to aspirate any of the middle layer. The layer is transferred into a fresh sterile eppendorf tube. Adding 0.5ml of isopropanol and 1 μl of linear acryl amide to precipitate out the RNA. The samples are then shaken and incubated for 10 minutes

on ice and then centrifuged as before for 10 minutes. A pellet should be visible at this stage. The supernatant is discarded without taking up the pellet. 1ml of 75% ethanol is added. The tube is briefly vortexed and centrifuged for 10 minutes. Then all the ethanol in the eppendorf tube is removed and the pellet dried at 45°C for 1 minute or at room temperature for 10 minutes. The pellet is then resuspended in 10µl of DEPC treated H₂O and incubated at 55°C for 10 minutes.

2.4 cDNA synthesis

The cDNA synthesis reaction was prepared as follows using Invitrogen reagents

O i g o dT	1 µ l
5 x b u f f e r	4 µ l
DTT (0. 1M)	2 µ l
dNTPs	1 µ l
RNase i n h i b i t o r	0. 5 µ l
M L V - S u p e r s c r i p t	1 µ l
T e m p l a t e R N A	10 µ l

The samples were incubated at 65°C for 10 minutes and then cooled on ice for 1 minute. Then 9ul of mix was added to all samples and rapidly pelleted at 4°C. The samples were incubated at 42°C for 1 hour and then 90°C for 10 minutes on the heat block and cDNA was stored at -70°C.

2.5 Real-Time PCR

Step	Temperature	Duration	Cycle No.
1	50°	120 (sec)	1
2	95°	600 (sec)	40
3	95°	15 (sec)	
4	60°	60 (sec)	

2.6 Flow Cytometry

NIH3T3 cells were collected in FACS wash buffer and subsequently centrifuged at 4 °C for 4 minutes using a Heitich Rotana 460R centrifuge. Following this, the cell suspension was plated out to a round-bottom 96 well plate (NUNC, Denmark). Cells were then washed with 100µl FACS wash buffer and incubated at 4 °C for 30 minutes with primary antibody (Table 1.1), which was suspended in 50 µl FACS wash buffer. Following incubation, the cells were again centrifuged and washed with FACS wash buffer. If necessary, secondary antibody (Table 1.1) was added and incubated for 30 minutes at 4°C. These cells were subsequently washed with FACS wash buffer, resuspended in 50µl FACS wash buffer and transferred to cluster tubes (Costar, Corning, NY). Single color standards and unstained controls were also prepared for compensation of the flow cytometer. Data was collected on a FACS (BD Bioscience, San Jose, CA) and analyzed with Flowjo software (Treestar San Carlos, CA).

2.6.1 Antibodies used for Flow Cytometry

The following is a list of antibodies used in various flow cytometry experiments. Primary antibodies are classified by their conjugation to FITC, APC, PE or PerCP. In the case of biotin conjugated antibodies, a secondary antibodies stain is required: streptavidin (SA) - conjugated to a fluorochrome.

Ant i gen	Conj ugat i on	Di l ut i on	Vendor
Human CD4	APC	1: 50	CALTAG Labor at ori es
N A	7AAD	1: 200	Mbl ecul ar probes
Human ICCS	bi ot i n	1: 100	BD Phar m i ngen
Bi ot i n	PE	1: 2000	BD Phar m i ngen

2.7 Common buffers and chemicals

2.7.1 Phosphate Buffer Saline (PBS, prepared by JCSMR media services)

NaCl	8.0 g/L
Dī sodi um hydr ogen or t hosphat e	1.25 g/L
Sodi um di hydr ogen or t hosphat e (monohdr at e)	0.35 g/L

2.7.2 Tris- acetate-EDTA (TAE) electrophoresis Buffer

Tri s- acet at e	40 mM
EDTA	1 mM

2.7.3 EtBr staining Buffer

Et Br (10mg/ mL) (MFCSCQ Chi o)	200 μ l
ddH ₂ O	1 L

2.7.4 FACS Wash buffer

PBS	
Sodium Azide	0.1%
Fetal Calf Serum	2%

2.7.5 Agarose Gel Loading Dye

Bromophenol Blue	1 mg/ml
Glycerol	20%

2.7.6 5x Sequencing Buffer

Tris-HCl	400 mM
MgCl ₂	10 mM
pH 9.0	

2.7.7 Ampicillin Agar Culture Plate

LB broth (JCSMR media)	
Bacto Agar w/v (Becton Dickinson, Mountain View, CA, USA)	1.5%
Ampicillin (Boehringer, Mannheim, USA)	100 μ g/ml

2.7.8 Hepes Buffered Saline (HBS) buffer

HEPES (pH 7.4)	10 mM
NaCl	150 mM
EDTA	3.4 mM
Surfactant P20 (BIAcore)	0.005%

2.7.9 Luria-Bertani LB broth

Tryptone	1%
Yeast extract	0.5%
NaCl	1%

2.8 Statistical Analysis

Where appropriate, a two-tailed non-paired T test was performed where Gaussian distribution was not assumed (Mann-Whitney test). P-values denoting statistical significance were considered significant when less than 0.05 and marked with an asterisk (*). P-values considered extremely significant when less than 0.01 were marked with an asterisk (**). All statistical analysis was performed using Excel (Microsoft) and Graphpad Prism (GraphPad Software, San Diego, CA).

2.9 Bioinformatics tools

For this study, bioinformatics tools used are listed below:

Research. (http://frodo.wi.mit.edu/cgi-bin/primer3/primer3_www.cgi)

BLAST - searching sequence homology, NCBI.
(<http://www.ncbi.nlm.nih.gov>)

BLAST 2 Sequence - pair-wise alignment-based comparison of sequence, NCBI.
(<http://www.ncbi.nlm.nih.gov/>)

ENSEMBL - public mouse genome assembly, Mouse genome sequencing consortium. (<http://www.ensembl.org>)

VISTA - a comprehensive suite of programs and database for comparative analysis of genomic sequences,
(<http://genome.lbl.gov/vista/index.shtml>)

In chapter 2 we described a pathway of CD4⁺ T cells in which CD4⁺ T cells were shown to be involved in the regulation of ICOS expression. The expression of ICOS was shown to be regulated by CD4⁺ T cells in a CD4⁺ T cell-dependent manner.

§ THREE §

Icos 3'UTR is required to mediate Roquin's repression

Roquin is a protein that has been shown to be involved in the regulation of gene expression. It is a member of the BTB domain protein family and is known to interact with a number of transcription factors. In this chapter, we investigated the role of the *Icos* 3'UTR in the regulation of Roquin's repression. We found that the *Icos* 3'UTR is required for Roquin to mediate its repression of *Icos* expression.

There is considerable evidence to suggest that the ICOS-ICOSL pathway appears to be primarily involved in the formation of germinal centers. In addition, it is known to be involved in the regulation of cell survival. This is likely due to the fact that ICOSL is a costimulatory molecule that is expressed by DCs. In this chapter, we investigated a direct role for ICOSL in the regulation of the ICOS pathway. We found that ICOSL is required for the activation of the ICOS pathway. We also found that ICOSL is required for the regulation of Roquin's repression of *Icos* expression. We found that the *Icos* 3'UTR is required for Roquin to mediate its repression of *Icos* expression. We found that the *Icos* 3'UTR is required for Roquin to mediate its repression of *Icos* expression. We found that the *Icos* 3'UTR is required for Roquin to mediate its repression of *Icos* expression.

3. 1 Introduction

In *sanroque* mice there is a striking overexpression of ICOS on CD4⁺ T cells in both naïve (CD44^{low}) and memory/activated (CD44^{high}) populations compared to their wild-type counterparts (Fig. 3.1A) (Vinuesa *et al.*, 2005a). The aberrant expression of ICOS caused by the M199R mutation in Roquin is intrinsic to T cells: in 50%:50% mixed bone marrow chimera experiments only T cells derived from the *san/san*, but not wild-type bone marrow displayed high expression of ICOS. These data suggest Roquin acts in T cells to repress ICOS expression.

When *sanroque* mice were crossed with TCR^{HEL}:insHEL double transgenic mice, 100% of *san/san*: TCR^{HEL}:insHEL mice became diabetic by 3-7 weeks of age, and ~ 60% of *san/+*:TCR^{HEL} mice also developed diabetes with slightly delayed onset. In these mice, diabetes was accompanied by very high titers of anti-HEL IgG autoantibodies and robust germinal-center reactions within the pancreas and draining lymph nodes, suggesting a profound failure to control T-cell help to self-reactive B cells in *sanroque* mice (Vinuesa *et al.*, 2005a). When gene expression was compared between purified *san/san* and *+/+* CD4⁺ T cells, there was a subset of genes that were more highly expressed in *sanroque* T cells. This included molecules important for successful T: B cell interactions in germinal centres, such as *IL-21*, *ICOS*, *CXCR5* and *CXCL13* (Vinuesa *et al.*, 2005a) (Figure 3.1B).

There is considerable evidence to suggest the ICOS: ICOSL pathway appears to be particularly important for the formation of germinal centers, the selection of memory B cells, and probably for the maintenance of self tolerance. Only recently, studies by Di Yu in our laboratory have confirmed a direct role for ICOS overexpression in the pathogenesis of the lupus syndrome in *sanroque* mice (Yu *et al.*, 2007). I then set out to investigate the mechanism by which Roquin regulates ICOS expression. We already knew that *Icos* mRNA levels were increased in *sanroque* mouse T cells (Figure 3. 1B), thus it was unlikely that ICOS overexpression was due to post-translational regulation (i.e. ubiquitin-mediated degradation). Our starting question was whether this regulation was occurring at a transcriptional or post-transcriptional level. We had several important clues that together suggested Roquin might be involved in post-transcriptional regulation of *Icos* mRNA:

- 1) Roquin's CCCH type zinc finger motif has been unequivocally shown to directly bind to RNA sequences found in the 3'UTR of target genes (Hudson et al., 2004; Kashanchi and Brady, 2005). This alone suggests Roquin might be a RNA-binding protein.
- 2) Roquin localizes to SGs. SGs are sites where mRNAs are sorted and stored in a translationally-inactive state, and many of them directed to processing bodies (PBs) for degradation (Anderson and Kedersha, 2006). Thus it is possible that Roquin acts on *Icos* mRNA to influence its stability or translation.
- 3) *Icos* mRNA contains a very long 3' untranslated region (UTR), which is over three times the size of the coding sequence (CDS) and has six areas that are as highly conserved as the coding region with over 70% homology in 100 bps (Figure 3.2). Many regions, particularly those that are AU-rich, found in transcripts containing long 3'UTRs have been shown to contain regulatory elements for mRNA stability, translation and localization (Zhang et al., 2007).
- 4) Co-transfection of HEK 293T cells with a construct expressing Roquin and another construct expressing ICOS either in its full length form (*hulcos*^{FL}), or lacking the 3'UTR (*hulcos*^{CDS}) showed Roquin repressed ICOS expression only when *Icos* mRNA contained the 3'UTR (Figure 3.3) (Yu et al., 2007). Unfortunately these results were not very consistent and were hard to quantify, partly due to using transfection into HEK293T cells (see below).

In the first part of this chapter, I will describe a new method I set up with the help of Di Yu to perform these regulatory studies- a retrovirus-mediated system of NIH3T3 cell transduction. In the rest of this chapter and subsequent two chapters, I have applied this system to identify the *cis*-acting elements in two different Roquin target genes, *Icos* and *Tnf*.

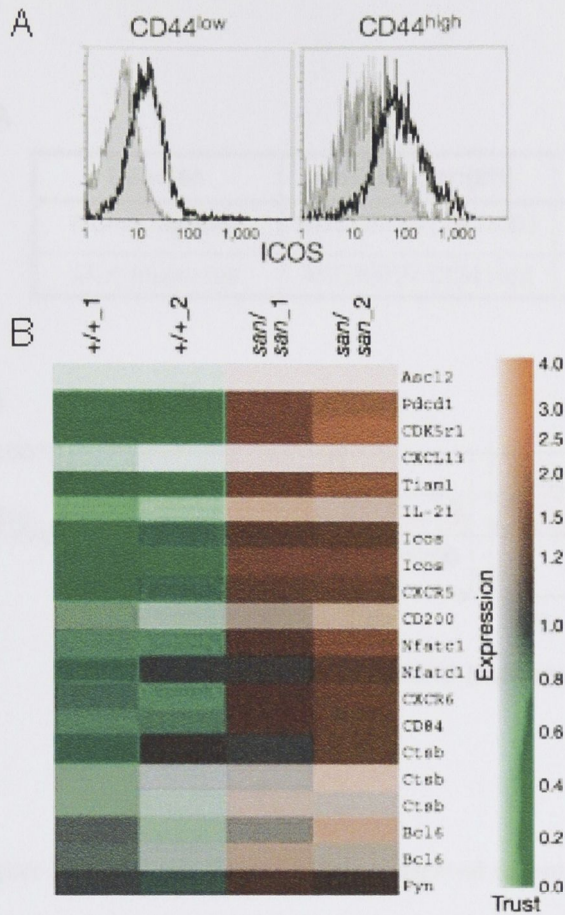


Figure 3.1

- A. ICOS expression on naïve (CD44^{LOW}) and activated/ memory (CD44^{high}) CD4⁺ T cells from *sanroque* mice (*san/san*, open histogram) and from wild-type mice (+/+, shaded histogram).
- B. Expression of T_{FH}-associated genes in purified CD4 splenic T cells from 12-weeks old *san/san* mice compared with +/+ littermates using Affimetrix microarrays. Two replicas are shown.

Reproduced from: Vinuesa, C.G. *et al.* Nature 435,452-8(2005).

A

Species	RefSeq (length)	CDS (length)
<i>Homo sapiens</i>	BC028210 (2651bp)	36-635 (600bp)
<i>Mus musculus</i>	AK030827 (3241bp)	39-641 (603bp)

B

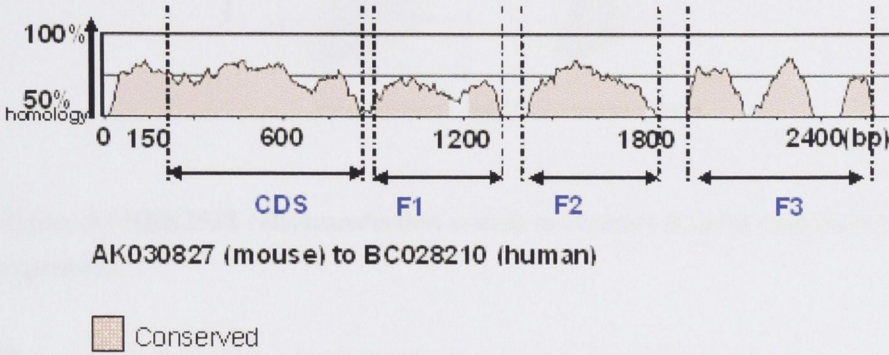


Figure 3.2 *ICOS* mRNA has highly conserved regions within 3'UTR

- A. The indicated human and mouse *ICOS* full length nucleoclide sequence (cDNA) were chosen from the GenBank database.
- B. Human and mouse *Icos* nucleoclide sequence were aligned using LAGAN (VISTA server <http://genome.lbl.gov>). Areas filled in pink represent conserved regions with more than 70% homology across 100 bps.

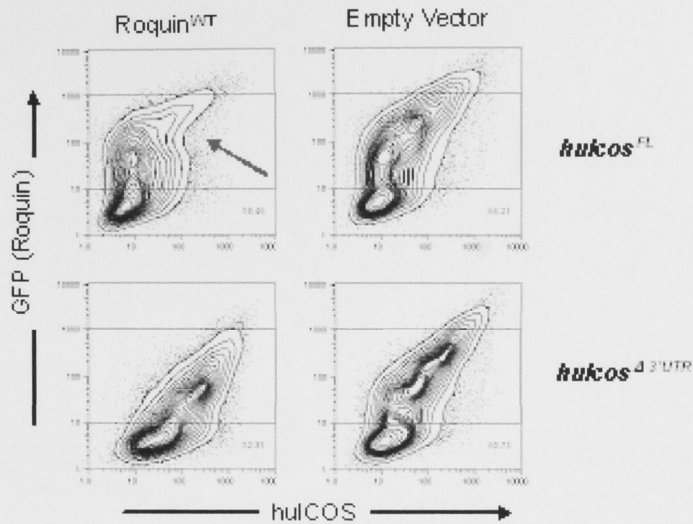


Figure 3.3 HEK293T cells transfection system to evaluate Roquin's repression of ICOS expression.

Flow cytometric analysis of HEK293T cells transfected with two constructs:

- 1) Roquin or empty vector – tagged with GFP
- 2) huIcos FL or huIcos $\Delta 3'$ UTR

Each combination is shown above as a separate dot-plot.

Contour-plot show GFP vs huIcos expression on each HEK293T cell population.

Repression of huIcos by Roquin was only observed when huICOS was expressed from full length *huIcos* (*huIcos*^{FL}) vector and is indicated with an arrow.

Di Yu performed these preliminary experiments using HEK293T cells

Fig. 3.4

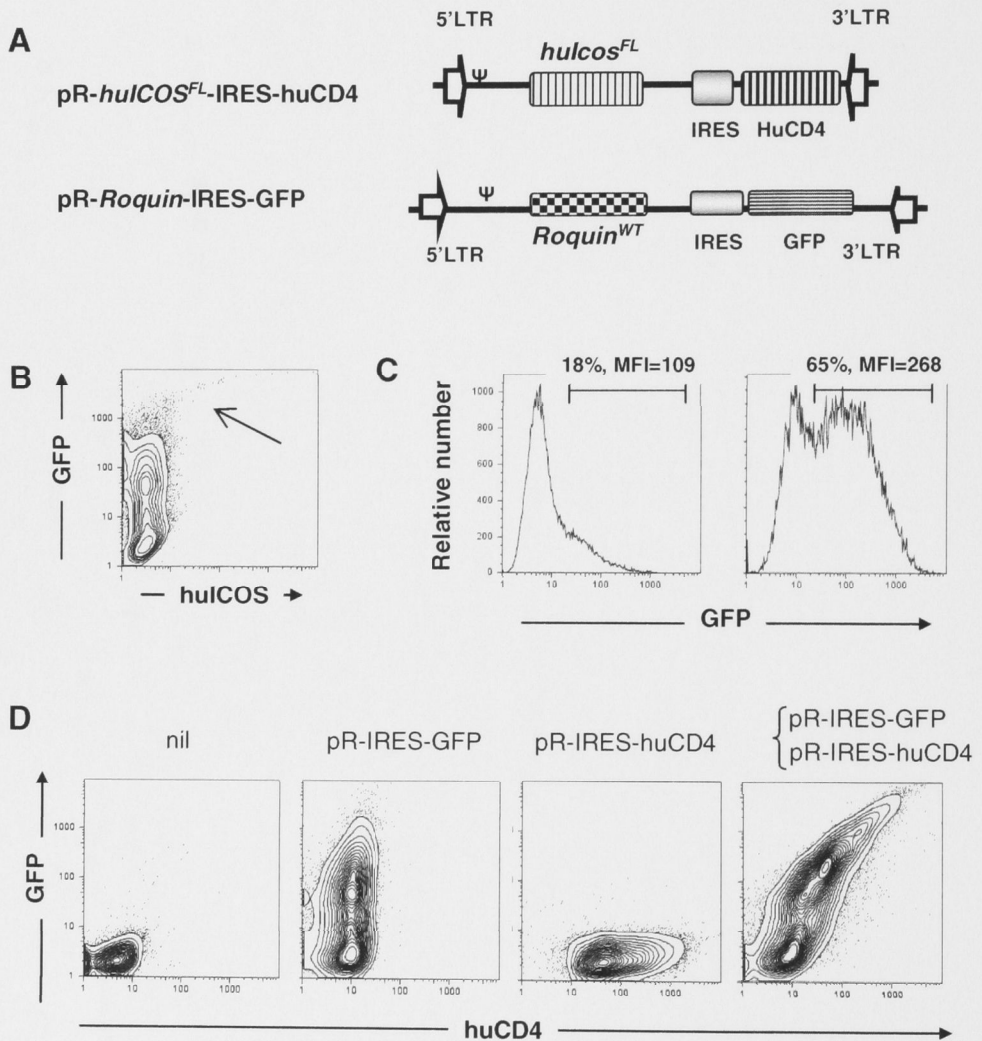


Figure 3.4 Disadvantages of using HEK293T cell transfection

- A. Schematic diagram of the vectors used to transfect *Icos* and *Roquin* into HEK293T cells.
- B. Flow cytometric analysis of HEK203T cells singly transfected with the pR-Roquin-IRES-GFP vector. Contour plot showing the fluorescence detected in FL1 and FI2 channels. There are cells expressing GFP with a fluorescent intensity over 1,000 units, leaking into FL2 channel (arrow).
- C. Histograms show mean fluorescent intensity (MFI) of GFP in HEK203T cells transfected with the pR-Roquin-IRES-GFP vector, with different efficiency. Left experiment in which there is low transfection efficiency. Right experiment in which there is high transfection efficiency.
- D. Contour plots of single or double transfected HEK293 with the vectors indicated (labels on top) showing GFP vs huCD4 fluorescence.

Di Yu performed these preliminary experiments using HEK293T cells

3.2 Development of a retrovirus-mediated transduction system to investigate the regulation of target mRNA by Roquin

When HEK293T cells were co-transfected with the constructs shown in Figure 3.4 to investigate Roquin's repression of ICOS, a few important problems were observed:

1. A fraction of the cells are highly transfected and express excessively high levels of reporter protein (GFP) resulting in fluorescent interference (i.e. FL1 fluorescence leaking into FL-2, Figure 3.4B).
2. Varying transfection efficiencies with different constructs makes it difficult to quantify gene-dose dependent effects (Figure 3.4C).
3. High correlation between the efficiency of transfection between two constructs makes interpretation of the data very difficult (Figure 3.4D). For our experiments it is very useful to have control cell populations expressing high amounts of one construct and low (or ideally nil) amounts of the other construct. This was never observed in experiments using HEK293T cell transfection.

For all of the above reasons we decided to establish a retrovirus-mediated gene transduction system into NIH3T3 cells. This system has the following advantages:

1. The transduction efficiency correlates very well with the concentration of retroviral particles present in the supernatant (Figure 3.5A).
2. The relationship between transduction efficiency and amount of retroviral supernatant can be calculated using a trend line fitted to the experimental data (Figure 3.5B).
3. This allows virus titration, and calculation of the optimal concentration that leads to comparable and constant transduction efficiencies across the different constructs (Figure 3.5C).

Fig. 3.5

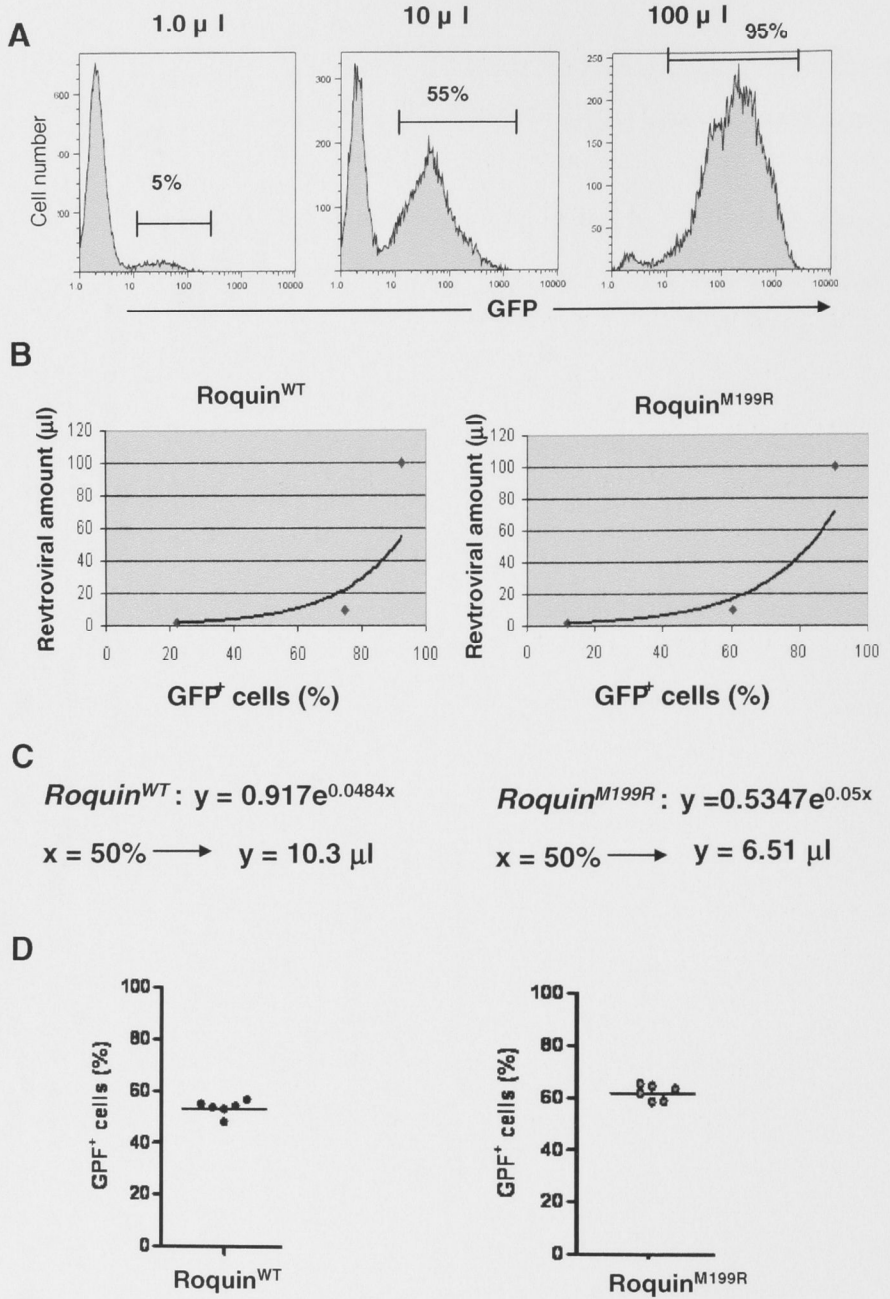


Figure 3.5 Explanation of the method used to titrate retrovirus –containing supernatant

- A.** Flow cytometry analysis of NIH3T3 cells transduced with the indicated volumes of a retrovirus-containing supernatant. Histograms indicate GFP fluorescence of transduced cells. The percentages of GFP positive cells shown are an indicator of transduction efficiency.
- B.** Dot plots showing the amounts of retrovirus-containing supernatant in a logarithmic scale (Y-axis) vs the percentage of transduced cells in a linear scale (X-axis). Trend lines were added to estimate viral titres. Left: Retrovirus expressing Roquin^{WT}; right: retrovirus expressing Roquin^{M199R}.
- C.** The equation predicted by each trend line is used to calculate the amount of retrovirus-containing supernatant required to achieve 50% transduction efficiency.
- D.** Flow cytometric analysis of NIH3T3 cells transduced with the amounts of retrovirus-containing supernatant. Dot blots show the % of GFP⁺ cells after one transduction; each symbol represents a separate population of transduced cells (transduced separately). Lines are drawn through the median values for each group. The transduction efficiencies of NIH3T3 cells transduced with Roquin^{WT}-(left) and Roquin^{M199R}-(right) expressing retroviruses were compared in parallel.

This NIH3T3 system was developed under the guidance of Di Yu.

My contribution to these experiments is estimated to be ~80%.

3.3 The 3'UTR, but not the coding region within *Icos* mRNA is required for Roquin's regulation

I set out to confirm the finding that the repression of ICOS expression by Roquin requires 3'UTR of *Icos* mRNA using retrovirus-mediated transduction of NIH3T3 cells. I generated the following constructs (Figure 3. 6):

- *huIcos*^{FL}: huICOS full length cDNA, subcloned into the multiple cloning site upstream of the IRES in the retroviral vector pR-IRES-huCD4
- *huIcos*^{CDS} huICOS cDNA lacking the 3'UTR and 5'UTR, subcloned into the multiple cloning site upstream of the IRES in the retroviral vector pR-IRES-huCD4.
- *Roquin*^{WT} cDNA mouse sequence was subcloned into the multiple cloning site upstream of the IRES in the retroviral vector pR-IRES-GFP.
- *Roquin*^{M199R} cDNA mouse sequence was subcloned into the multiple cloning site upstream of the IRES in the retroviral vector pR-IRES-GFP.

A retroviral supernatant from each individual retroviral construct was harvested from Phoenix cell cultures (the packaging cell line) and titrated to achieve about 50%-60% transduction for each retrovirus under the same conditions (spinoculation at 30°C and 2500rpm for 90minutes). NIH3T3 cells were co-transduced with supernatants from these constructs in the following combinations (Figure 3.7A)

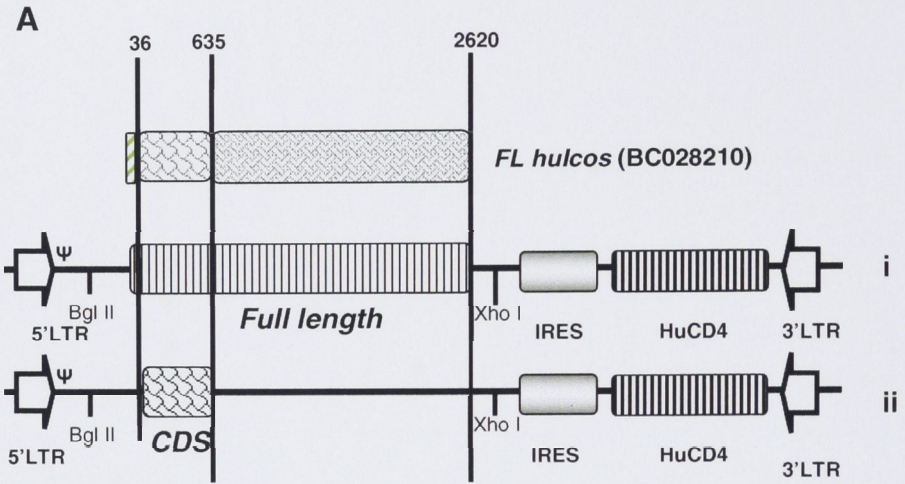
1. Either pR-*Roquin*^{WT}-IRES-GFP or pR- *Roquin*^{M199R}-IRES-GFP, or empty pR- IRES-GFP vector (also referred to as empty^{KMV-GFP})

Plus

2. pR-*huIcos*^{FL}-IRES-huCD4 or pR- *huIcos*^{CDS} -IRES -huCD4.

In these constructs, *huIcos* mRNA fragments were subcloned into the retroviral vector pR-IRES-huCD4, upstream of an internal ribosomal entry site (IRES) in the bicistronic message of *huIcos* cDNA. Thus, *huCd4* and *Icos* cDNAs are transcribed into a single transcript, although translation occurs independently. That means the huCD4 maker gene may also serve as a reporter maker for ICOS expression, if Roquin exerts its repression on the transcript (i.e. regulating mRNA abundance rather than translation).

Fig. 3.6



B

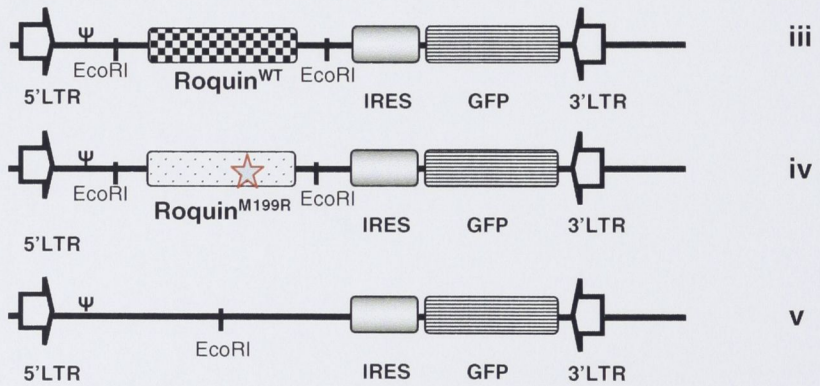


Figure 3.6 Schematic representation of the retroviral constructs.

A. The full length (FL) or coding sequence (CDS) of *hulcos* cDNA were inserted into the retroviral vector pR-IRES-huCD4 using the restriction enzymes Bgl II and Xho I. The number indicates the base pair position within the BC028210 sequence.

- (1) pR-huIcos^{FL}- IRES-huCD4
- (2) pR-huIcos^{CDS}- IRES-huCD4

B. Wild-type (Roquin^{WT}) and mutant (Roquin^{M199R}) *Roquin* cDNA were inserted into the retroviral vector pR-IRES-GFP using the restriction enzyme EcoR I.

- (1) pR-Roquin^{WT}-IRES-GFP
- (2) pR-Roquin^{M199R}-IRES-GFP
- (3) pR-IRES-GFP (empty vector control, also referred to as Empty^{KMV-GFP})

Fig. 3.7

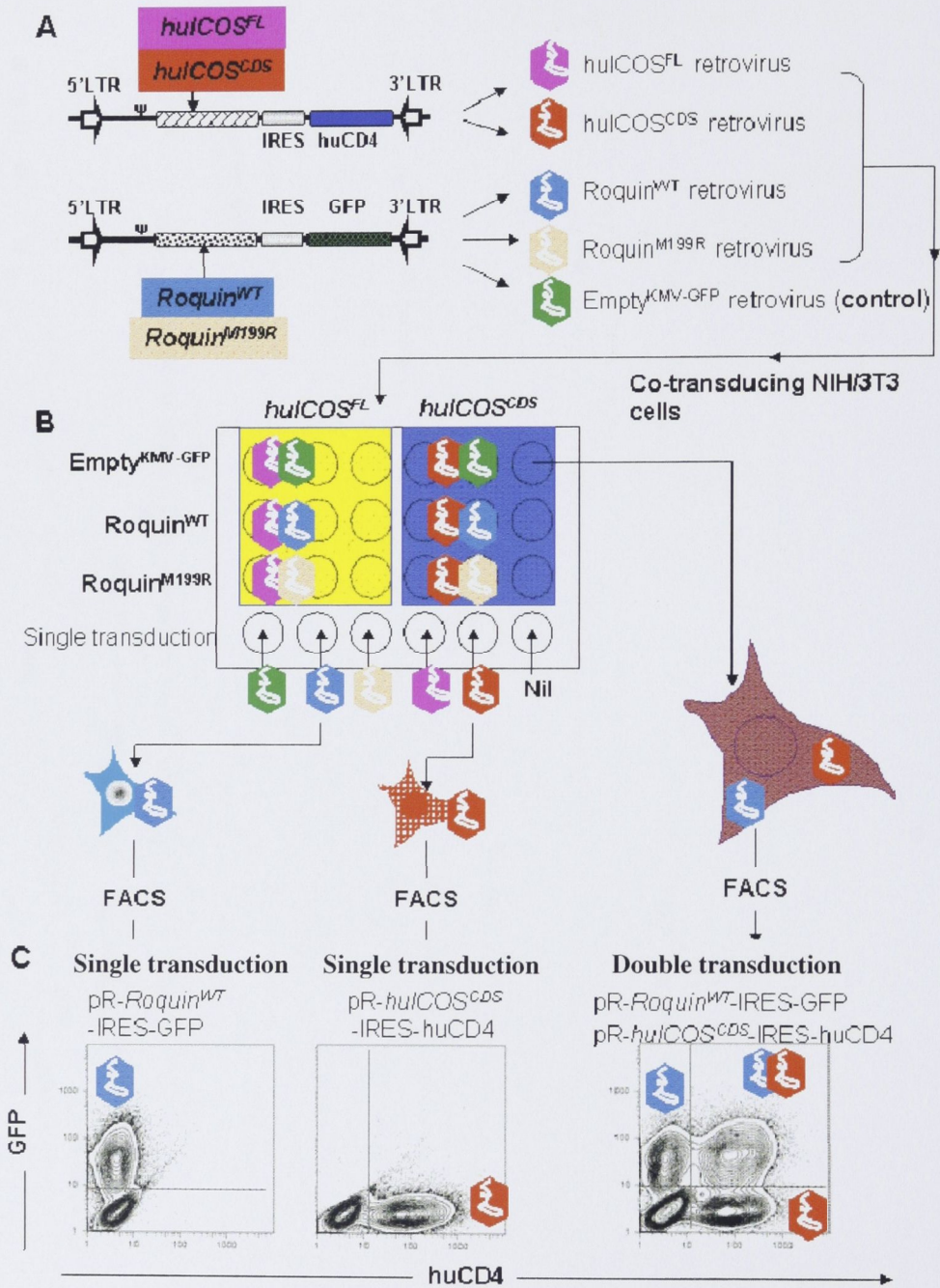


Figure 3.7 Flow chart summarises the experiment plan for the retrovirus-mediated gene transduction of NIH3T3 cells

- A.** Retroviruses packaged from the constructs shown in Fig. 3.6.

- B.** After titration, the selected amount of retrovirus was used to transduce cells seeded in the 24-well plates. The different combinations of the retroviruses that were used for transduction are shown. Double transduction experiments were always performed in triplicate and then repeated in a separate experiment. Single transductions were performed in order to calibrate the flow cytometer and establish the compensation settings.

- C.** Representative flow cytometry contour plots showing singly transduced and doubly transduced cells.

Two days after transduction, NIH3T3 cells were analyzed by flow cytometry (Figure 3.7B/C). The gating strategy used for this analysis is shown in Figure 3.8 and 3.9.

1. A live cell gate was first placed according to size (forward scatter) and granularity (side scatter) (Figure 3.8A).
2. Dead cells were excluded from analysis by gating only cells that were 7AAD^{low} (Figure 3.8B).
3. GFP versus ICOS fluorescence was plotted to observe the effect of Roquin on ICOS expression since Roquin was expressed from a bicistronic vector also expressing GFP (Figure 3.8C).
4. Cells were divided into three populations: Roquin^{Hi} (GFP^{Hi}), Roquin^{Low} (GFP^{Low}) and Roquin^{Nil} (GFP^{Nil}), according to the level of GFP expression (Figure. 3.9A). The method used to quantify Roquin-mediated repression of ICOS is explained in figure 3.9B.

After performing the analysis described above, I quantified the level of ICOS repression by the different Roquin vectors expressing ICOS expression levels as the percentage of the level seen in cells transduced with the empty pR-IRES-GFP construct.

Roquin^{WT} exerted a potentially inhibitory effect on huICOS expression when cells were co-transduced with the *huICOS^{FL}* construct, containing the 3'UTR. Indeed, a high dose of Roquin^{WT} repressed huCD4 expression to 45% and repressed huICOS expression to 25% of the levels found in cells transduced with the empty-GFP vector. A comparable dose of Roquin^{M199R} repressed huCD4 expression to 60% and huICOS expression to 45%. A low dose of Roquin^{WT} repressed huCD4 expression to 75% and huICOS expression to 70%, while Roquin^{M199R} repressed huCD4 expression to 80% and huICOS expression to 90%. In cells lacking Roquin expression, there was no significant repression of huCD4 or of huICOS (Figure 3.10). These results show that the cells with highest GFP expression – indicating a higher gene dose of Roquin – exert a more potent repressive effect compared to cells with low levels of Roquin expression. This is an important result that indicates Roquin represses ICOS expression in a gene-dose dependent manner. Moreover, as predicted, the Roquin^{M199R} mutation was less capable of repressing huCD4 and huICOS expression, which confirms this mutation diminishes but does not abolish Roquin's function.

Roquin^{WT} could not down-regulate ICOS expression when cells were co-transduced with huICOS CDS lacking huICOS3'UTR (figure 3.10). This result confirmed Di Yu's previous finding using the HEK293T cells system, of Roquin repressing ICOS expression through its 3'UTR.

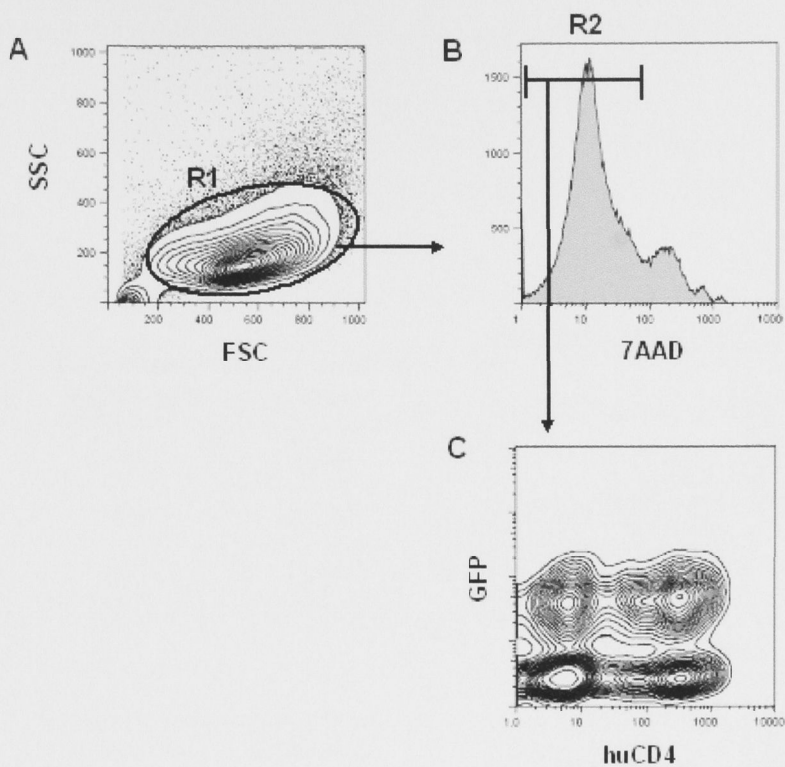
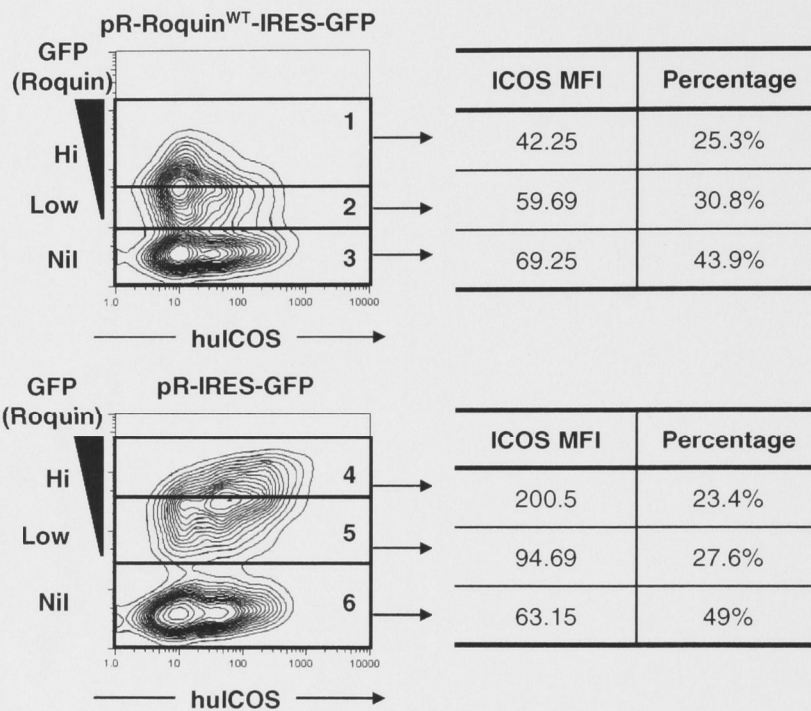


Figure 3.8 Gating strategies for the flow cytometric analysis.

- A.** Region one (R1) was placed based on size (forward scatter) and granularity (side scatter) to gate live cells and eliminate dead cells and/or debris.
- B.** R2 was placed on the cell population gated in R1, to exclude dead cells that are 7AAD positive.
- C.** Cells from R2 were plotted as contour plots showing GFP *versus* huCD4 (or ICOS where indicated).

Fig. 3.9

A



B

Roquin level	Calculation	Relative expression
High	$\frac{42.25}{200.5}$ (#1 / #4)	21%
Low	$\frac{59.69}{94.69}$ (#2 / #5)	70%
Nil	$\frac{69.25}{63.15}$ (#3 / #6)	110%

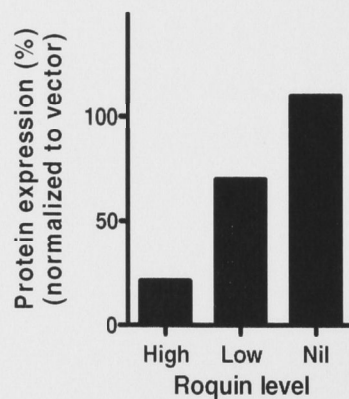


Figure 3.9 Quantification of Roquin-mediated repression.

- A.** Retroviral titres were determined to consistently achieve a transduction efficiency of 50-60% of NIH3T3 cells. Upper panel: cells transduced with Roquin-expressing retroviruses. Lower panel: cells transduced with empty vector. For cells transduced with Roquin (thus GFP⁺), the half with higher GFP expression was defined as the Roquin^{Hi} population (Gate 1), while the half with lower GFP expression was defined as Roquin^{Low} population (Gate 2). Cells that were not transduced are shown in gate 3 (these cells are referred to in the text as Roquin^{Nil}/GFP^{Nil}). Similar gates were placed in the empty-vector transduced cells (gate 4, 5, 6). The MFI of ICOS in each population is shown.
- B.** The MFI of ICOS in populations with different levels of Roquin transduction was normalized to the counterpart population from cells transduced with empty vector (pR-IRES-GFP).

This method of quantification using the retrovirus-mediated gene transduction cell system was developed by Di Yu.

3.4 Summary

In this chapter, we developed a retrovirus-mediated NIH3T3 cell system to investigate the regulation of ICOS expression by Roquin. This system allows quantification due to the possibility to control for transduction efficiency of the different constructs.

The experiment performed shows ICOS expression is most potently repressed in those cells that are transduced with the highest levels of exogenous Roquin, indicating repression occurs in a Roquin dose-dependent manner. The same Roquin dose-dependent repression was also observed for huCD4 expression.

Importantly, mRNA repression was only observed when ICOS was expressed from transcripts containing the 3'UTR, indicating this region contains *cis*-acting element(s) critical for Roquin-mediated regulation.

Finally, Roquin^{M199R} was unable to repress either ICOS or huCD4 expression to the levels seen with Roquin^{WT}, but did exert some inhibitory effect adding further evidence to the suggestion this is a hypomorph rather than a null allele.

Together these results show *Icos* mRNA 3'UTR is required for the repression of ICOS expression by Roquin and impaired 3'UTR-mediated repression might be the cause of ICOS overexpression on *sanroque* CD4⁺ T cells.

Fig. 3.10

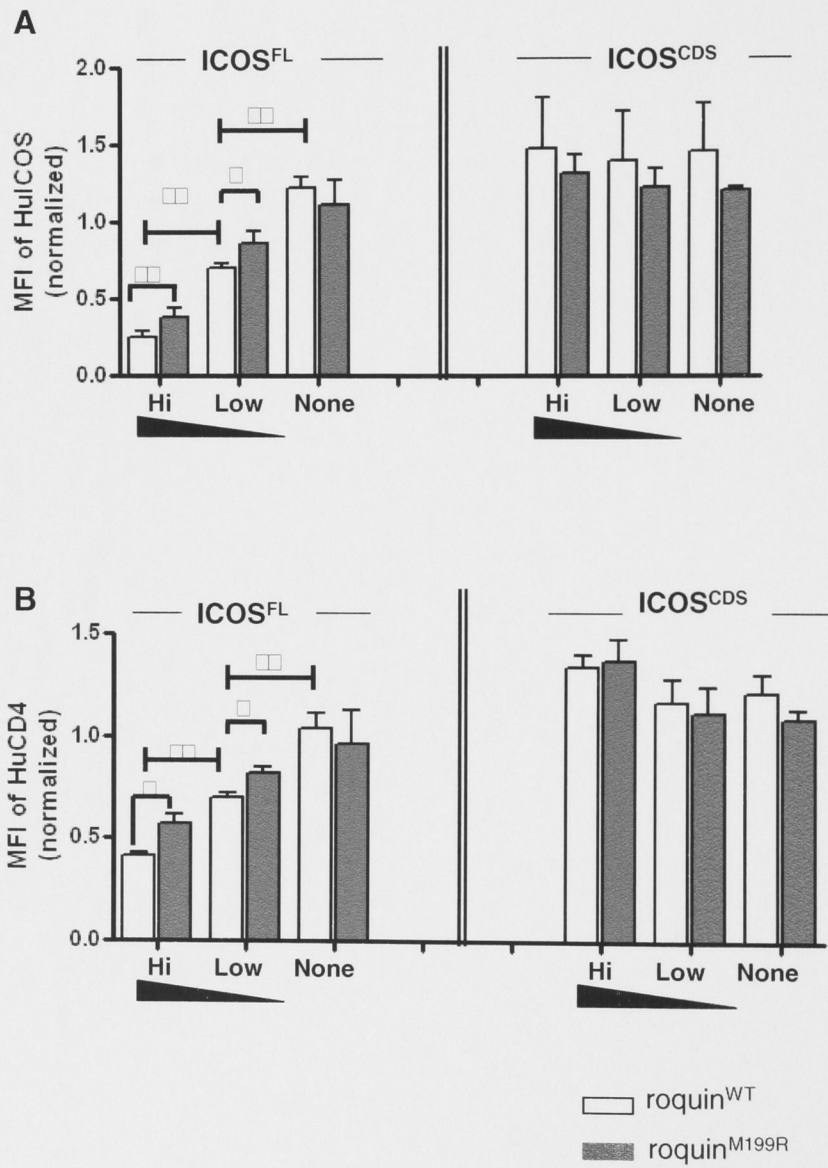


Figure 3.10 Repression of ICOS expression by Roquin requires 3'UTR in *ICOS* mRNA .

- A.** NIH3T3 cells were transduced with two retroviruses: one expressing either *hulcos*^{FL} or *hulcos*^{CDS}; the other expressing Roquin^{WT}, Roquin^{M199R} or empty vector as indicated. The repression of *hulcos* expression by either Roquin^{WT} or Roquin^{M199R} was quantified using the method described in Fig 3.11. The bars show the normalized MFI of huICOS in cells with different levels of Roquin^{WT} (open bars) or Roquin^{M199R} (filled bars) expression.
- B.** In this experiment huCD4 MFI is measured since huCD4 is downstream of *hulcos* in the bicistronic vector (see Fig 3.6a). The repression of huCD4 expression by either Roquin^{WT} or Roquin^{M199R} was quantified using the method described in Fig 3.9. Open bars represent cells expressing Roquin^{WT} and filled bars represent cells expressing Roquin^{M199R}.

Data shown represent mean value \pm S.D with n=3. Student's test *P<0.05; **P<0.01.

The results presented in this chapter demonstrate that the 3' UTR of *Icos* mRNA is the regulatory region for Roquin-mediated mRNA decay. The distal fragment within the 3' UTR contains the *cis*-acting element(s) and promotes Roquin-mediated *Icos* mRNA decay.

§ FOUR §

The distal fragment within *Icos* 3'UTR contains the *cis*-acting element(s) and promotes Roquin-mediated *Icos* mRNA decay.

4.1 Introduction

The results provided in the previous chapter have shown that the long 3'UTR of *Icos* mRNA is the regulatory region that mediates Roquin's repression. We next set out to try and identify which are the responsible *cis*-acting element(s) within *Icos* mRNA 3'UTR. Different *cis*-acting elements have been shown to regulate mRNA through different mechanisms; typically, AU-rich elements (ARE) mediate mRNA decay (Gingerich *et al.*, 2004), while for example micro-RNA (miRNA) target sequences predominantly regulate translation (Bartel, 2004). It then emerges that identification of regulatory elements may provide important information as to Roquin's mechanism of regulation. In most cases, *cis*-acting element(s) for mRNA regulation are no longer than 100 bp and can be predicted by bioinformatic analysis that identifies sequence patterns (Pesole *et al.*, 2002). The unusual length of the 3'UTR of *huIcos* mRNA - over 2kb long - greatly increases the possibility of false positive results using this approach. We decided to first identify a smaller region of *huIcos* 3'UTR responsible for the repressive effect, and only then use bioinformatic tools to predict the regulatory element(s).

Due to their physiological role in regulating gene expression, *cis*-acting elements in untranslated sequence tend to maintain their critical sequence patterns through evolution. Therefore, they are often in the core of the conserved regions across species. By performing a BLAST alignment between human and mouse *Icos* 3'UTR, we could identify six highly conserved regions (Figure 3.2). We then divided the 3'UTR into three fragments, with the criteria that they should be roughly of comparable size; each of them should contain one or more such conserved regions; and the boundaries between each fragment should not interrupt any conserved sequence (Figure 4.1A).

- Fragment one (F1) comprises conserved regions □ 2 and □ 3, with a length of 713 bp (from 635 to 1348, BC028210);
- Fragment two (F2) comprises conserved region □ 4, with a length of 535 bp (from 1349 to 1884, BC028210);
- Fragment three (F3) comprises conserved regions □ 5, □ 6 and □ 7, with a length of 766 bp (from 1885 to 2651, BC28210).

Fig. 4.1

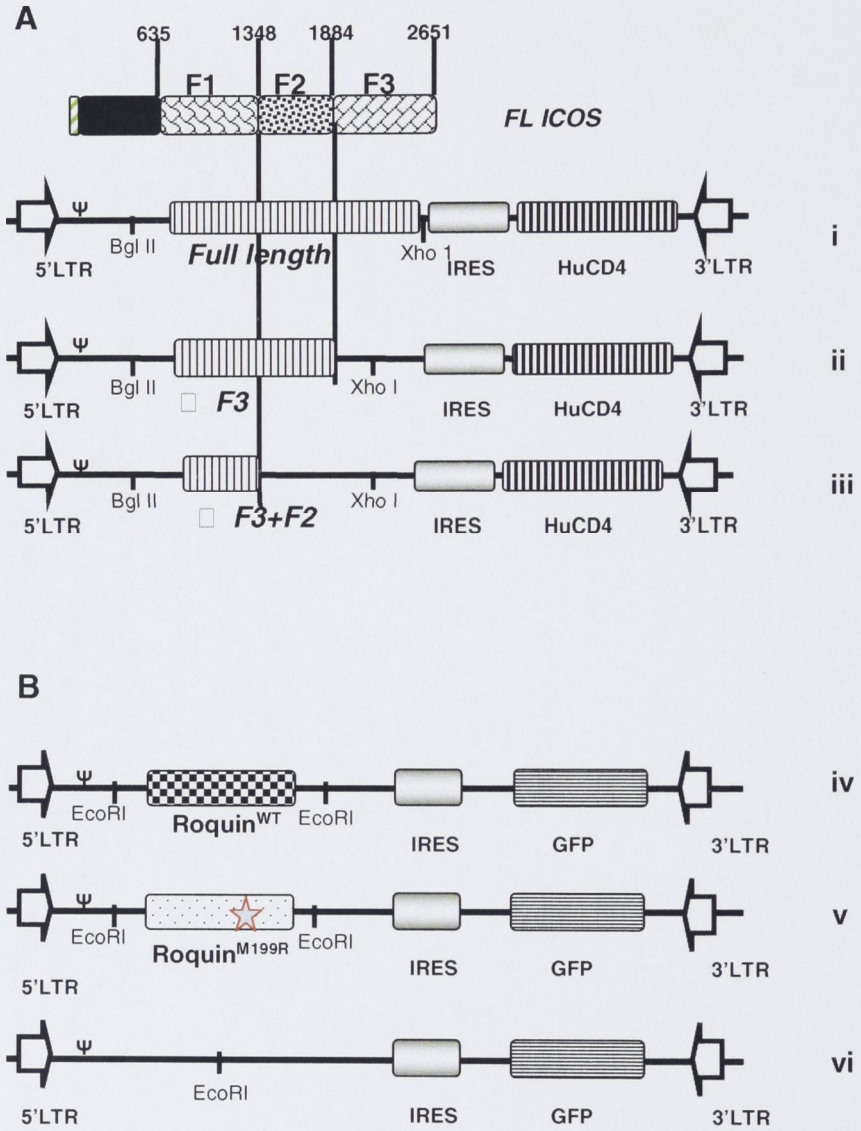


Figure 4.1 Schematic representation of the retroviral constructs.

A. The following *hulcos* fragments were inserted into the retroviral vector pR-IRES-huCD4 using the restriction enzymes Bg II and Xho I or Δ F3+F2, lacking F3+F2 *hulcos* cDNAs were.

- (1) pR-*hulcos*^{FL}-IRES-huCD4: Full length (FL) *hulcos* cDNA
- (2) pR-*hulcos* ^{Δ F3}-IRES-huCD4: *hulcos* cDNA lacking F3
- (3) pR-*hulcos* ^{Δ F3+F2}-IRES-huCD4: *hulcos* cDNA lacking F2 and F3

B. Wild-type (Roquin^{WT}) and mutant (Roquin^{M199R}) Roquin cDNAs were inserted into the retroviral pR-IRES-GFP vector using the restriction enzyme EcoR I.

- (1) pR-Roquin^{WT}-IRES-GFP
- (2) pR-Roquin^{M199R}-IRES-GFP
- (3) pR-IRES-GFP

4.2 F3 within 3'UTR is required for the repression of ICOS by Roquin

In order to test the requirement of each fragment for the repression of ICOS expression by Roquin, truncated forms of *hulcos* mRNA were constructed and subcloned into the retroviral vector pR-IRES-huCD4 used in the previous studies:

- *hulcos*^{ΔF3}: *hulcos* full length cDNA lacking the most distal fragment, F3, subcloned into the multiple cloning site upstream of the IRES in the retroviral vector pR-IRES-huCD4.
- *hulcos*^{ΔF3+F2}: *hulcos* full length cDNA lacking both F2 and F3, subcloned into the multiple cloning site upstream of the IRES in the retroviral vector pR-IRES-huCD4.

I then co-transduced NIH3T3 cells with retrovirus-containing supernatants from:

1. pR-Roquin^{WT}-IRES-GFP or pR-Roquin^{M199R}-IRES-GFP or pR-IRES-GFP empty vector;

Plus

2. pR-*hulcos*^{FL}-IRES-huCD4 or pR-*hulcos*^{ΔF3}-IRES-huCD4 or pR-*hulcos*^{ΔF3+F2}-IRES-huCD4 or pR-*hulcos*^{CDS}-IRES-huCD4.

In this double co-transduction, expression of ICOS could be assessed by measuring surface huICOS or huCD4 protein levels, and expression of Roquin could be assessed by GFP expression, using flow cytometry.

As shown in the previous chapter, both ICOS and huCD4 expression from *hulcos*^{FL} were potently repressed by Roquin^{WT} (Figure 3.10). By contrast, these levels of repression were not observed when ICOS and huCD4 were expressed from *hulcos*^{ΔF3}, *hulcos*^{ΔF3+F2} or *hulcos*^{CDS} although a subtle repression was still observed when ICOS was expressed from *hulcos*^{ΔF3}. Notably, when both F3 and F2 were absent from the *Icos* cDNA (*hulcos*^{ΔF3+F2}), no repression could be observed (Figure 4.2).

We also confirmed this repression was Roquin gene-dose dependent. Repression of both huCD4 and huICOS in cells transduced with *ICOS*^{FL} retrovirus was about 2-3 times higher in cells expressing high levels of Roquin (GFP^{Hi}) than in cells with low Roquin

Fig. 4.2

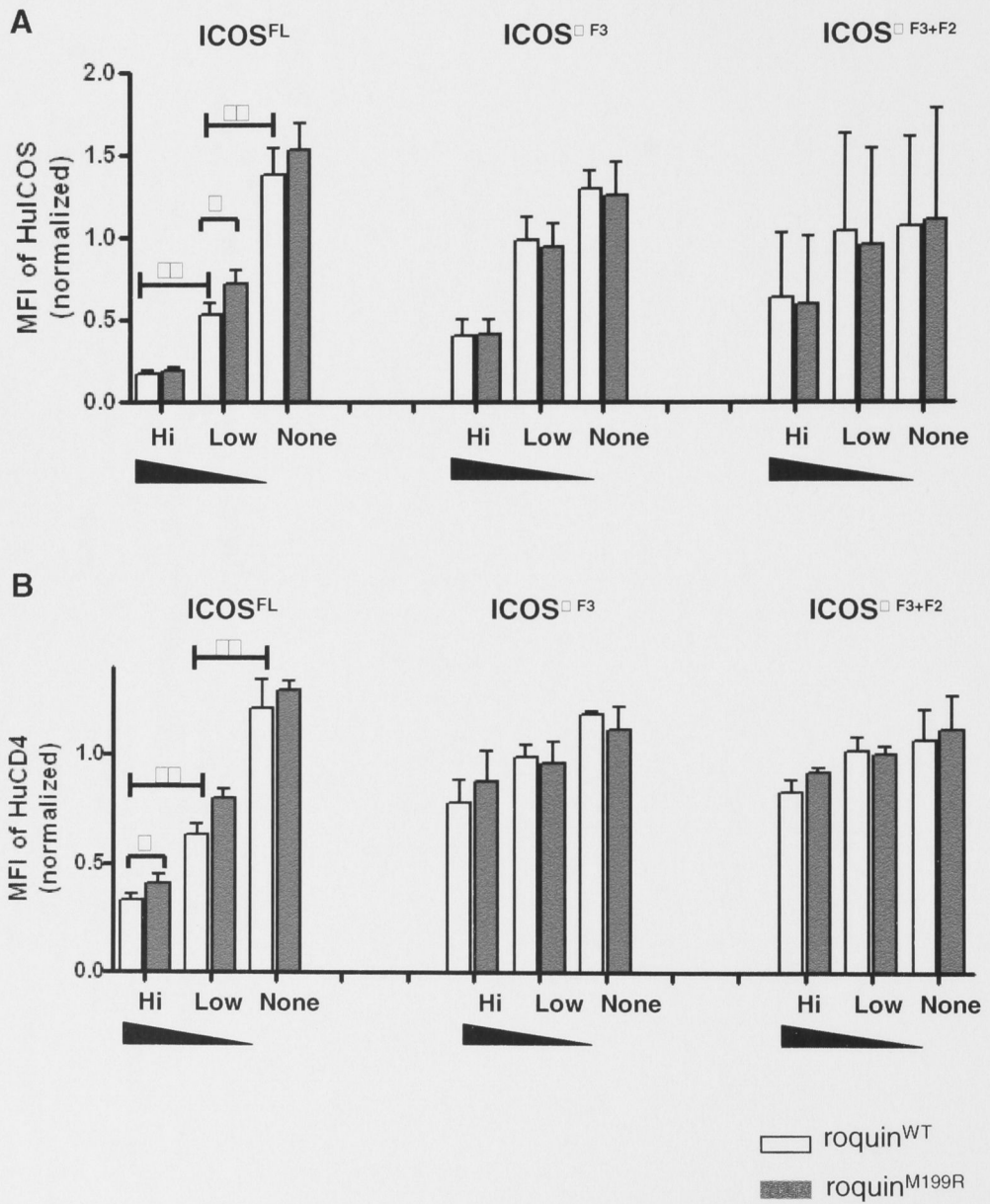


Figure 4.2 Repression of ICOS expression by Roquin requires the F3 fragment with *Icos* mRNA.

- A.** NIH3T3 cells were transduced with two retroviruses: one expressing ICOS from *huIcos*^{FL} or *huIcos*^{ΔF3} or *huIcos*^{ΔF3+F2}, the other expressing either Roquin^{WT} or Roquin^{M199R}. HuICOS expression was quantified using the method described in previous chapter.
- B.** Same experiment as A, but here, instead of ICOS, HuCD4 expression from the same bicistronic vector was measured. The repression of huCD4 expression by either Roquin^{WT} or Roquin^{M199R} was quantified using the method described in previous chapter.

Open bars represent Roquin^{WT} and filled bars represent Roquin^{M199R}. Data shown represent mean values ±S.D. with n=3. Student's test *P<0.05; **P<0.01.

levels (GFP^{L0}) (P<0.01 in huICOS; p<0.05 in huCD4) (Figure 4.2). By contrast, there were no differences between GFP^{Hi}, GFP^{L0} and GFP^{NIL} populations amongst cells transduced with ICOS^{□F3+F2} or ICOS^{□F3} (Figure 4.2)

All these results show that *hulcos-3'UTR-F3* is required for the repression of ICOS expression by Roquin. The logical next question is whether this F3 fragment is not only necessary but is also sufficient for this repression. Two possible scenarios are that i) F3 alone contains all the *cis*-acting regulatory element(s) or ii) F3 needs to interact with another element within a different 3'UTR fragment to mediate this repression.

4.3 F3 within 3'UTR is sufficient for the repression of ICOS by Roquin

In order to test whether F3 in *hulcos* mRNA 3'UTR is sufficient to mediate Roquin's repression, the effects of F1, F2 and F3 were tested separately. Since all previous experiments have proved that the expression of huCD4 is a good reporter for evaluating the repressive effect, the three 3'UTR fragments were individually subcloned into the pR-IRES-huCD4 retroviral vector (Figure 4.3A).

Next, NIH3T3 cells were co-transduced with supernatants from:

1. Either pR-Roquin^{WT}-IRES-GFP or pR-Roquin^{M199R}-IRES-GFP or pR-IRES-GFP empty vector;

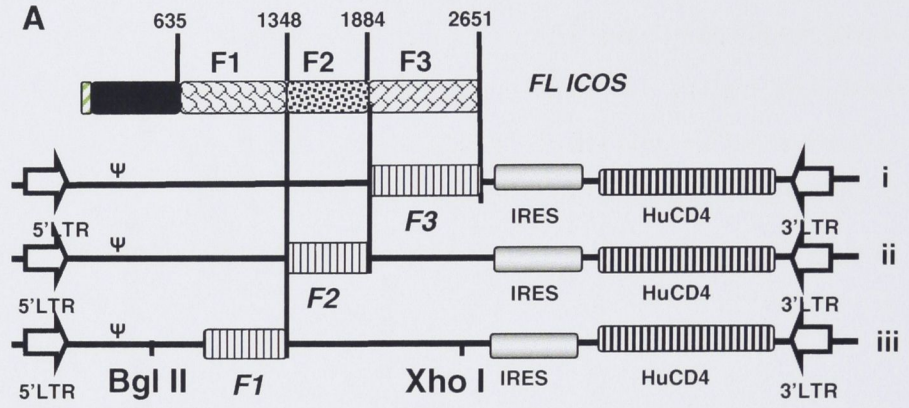
plus

2. Either pR-*hulcos*^{F1}-IRES-huCD4 or pR-*hulcos*^{F2}-IRES-huCD4 or pR-*hulcos*^{F3}-IRES-huCD4.

When we compared the repressive effects exerted by F1, F2 or F3, it became obvious that F3 alone could mediate all the suppressive effect (Figure 4.4). No repression of huCD4 expression could be observed in cells transduced with either *Icos-3'UTR-F1* or *Icos-3'UTR-F2*-expressing retroviruses (Figure 4.4).

The data above clearly show that F3 within *hulcos* mRNA 3'UTR is necessary and sufficient to mediate Roquin's repression. Importantly, the repression exerted by *Icos-3'UTR-F3* is comparable in potency to the repression exerted by the entire 3'UTR. This strongly suggests *cis*-acting element(s) are localised within *Icos-3'UTR-F3*.

Fig. 4.3



B

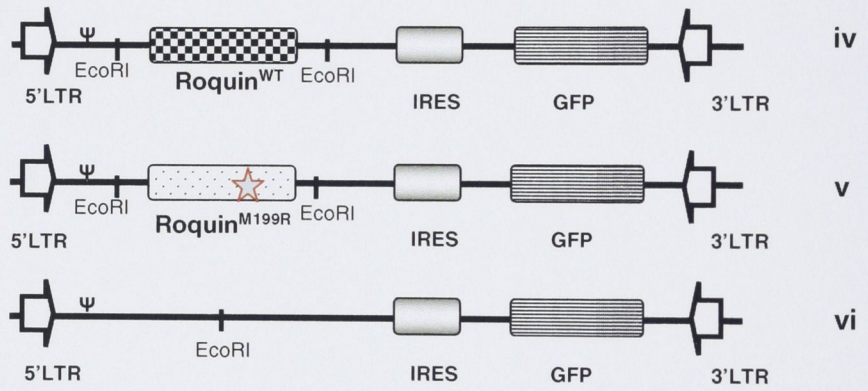


Figure 4.3 Schematic representation of retroviral constructs.

A. F3, F2 or F1 huIcos cDNA were inserted into the retroviral vector PR-IRES-huCD4 using the restriction enzymes BglII and XhoI.

(A) pR-huIcos^{F3}-IRES-huCD4

(B) pR-huIcos^{F2}-IRES-huCD4

(C) pR-huIcos^{F1}-IRES-huCD4

B. Wild-type (WT) and M199R mutant Roquin cDNA were inserted into the retroviral vector pR-IRES-GFP using the restriction enzyme EcoR I

(D) pR-Roquin^{WT}-IRES-GFP

(E) pR-Roquin^{M199R}-IRES-GFP

(F) pR -IRES-GFP

4.4 F3 within *Icos* 3'UTR mediates Roquin's promotion of mRNA degradation

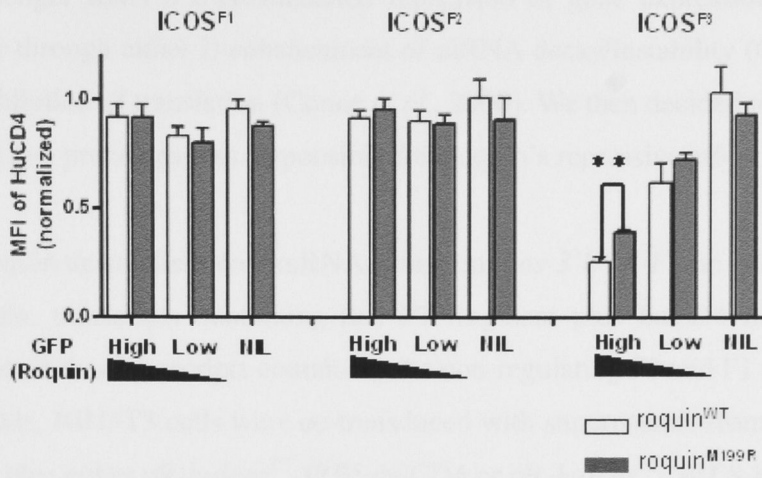


Figure 4.4 F3 within *Icos* 3'UTR is sufficient for Roquin's repression .

NIH3T3 cells were transduced with two retroviruses: one expressing ICOS from hu*Icos*^{F3} or hu*Icos*^{F2} or hu*Icos*^{F1}; the other expressing either Roquin^{WT} or Roquin^{M199R} or empty vector. The repression of huICOS expression by either Roquin^{WT} or Roquin^{M199R} was quantified in cells expressing high, low or null levels of Roquin (GFP).

Open bars represent Roquin^{WT} and filled bars represent Roquin^{M199R}. Data shown represent mean values \pm S.D. with n=3. Student's test *P<0.05; **P<0.01

4.4 F3 within *Icos* mRNA 3'UTR mediates Roquin's promotion of mRNA degradation

Messenger RNA 3'UTR-mediated repression of gene expression has been shown to occur through either i) enhancement of mRNA decay/instability (Conne *et al.*, 2000) or ii) inhibition of translation (Conne *et al.*, 2000). We then decided to investigate which of these two processes was responsible for Roquin's repressive effect on ICOS expression.

If Roquin destabilises *Icos* mRNA acting on *Icos*-3'UTR-F3, in cells co-transduced with Roquin, transcripts containing this F3 fragment plus huCD4 mRNA should be less abundant than transcripts containing the non-regulating F2 and F1 fragments. In order to test this, NIH3T3 cells were co-transduced with supernatants from pR-Roquin^{WT}-IRES-GFP plus either pR-*huIcos*^{F1}-IRES-huCD4 or pR-*huIcos*^{F3}-IRES-huCD4.

Two populations were separately sorted:

- i) Cells highly transduced with Roquin (GFP^{Hi})
- ii) Cells not transduced with Roquin (GFP^{Nil})

HuCd4 mRNA abundance was quantified by quantitative real-time RT PCR. The effect of each fragment (F1 or F3) on mRNA degradation can be determined by comparing mRNA abundance between Roquin^{Hi} and Roquin^{Nil} populations in cells transduced with *Icos*-3'UTR-F1-*huCd4* or cells transduced with *Icos*-3'UTR-F3-*huCd4*.

When *huCd4* mRNA was tagged with *Icos*-3'UTR-F1, there was no regulation of huCD4 expression regardless of the dose of Roquin (GFP) expression (Figure 4.4). However, in experiments where *huCd4* mRNA was tagged with *Icos*-3'UTR-F3, those cells with high levels of Roquin expression had more than a 3-fold decrease in *huCd4* mRNA transcripts compared to cells without exogenous Roquin expression (Figure 4.4). This can be seen in the figure as a repression of *huCd4* mRNA levels to 70-80% of the levels seen in cells lacking exogenous expression of Roquin (Figure 4.5B).

The results above show Roquin exerts a potent effect on ICOS mRNA decay acting through *Icos*-3'UTR-F3. The question remaining is whether all of Roquin's repressive

Fig. 4.5

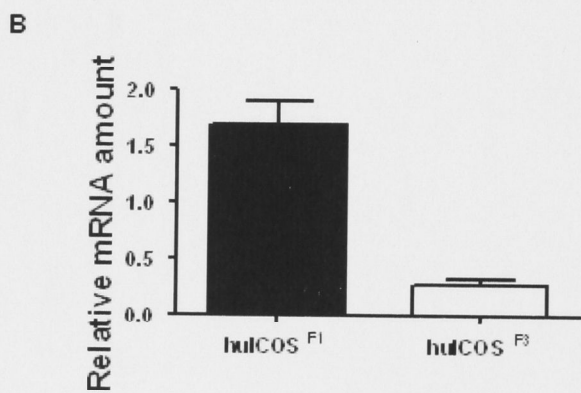
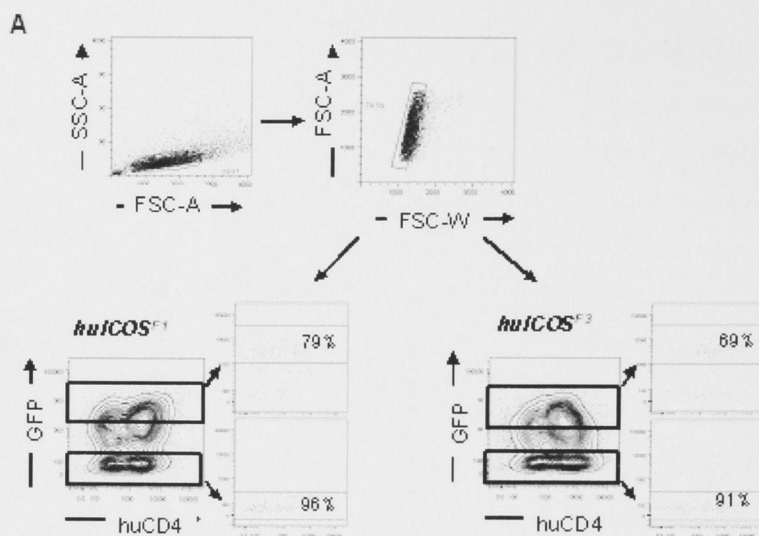


Figure 4.5 Roquin represses mRNA abundance through the F3 fragment within Icos 3'UTR

- A.** Gating strategy used to exclude cellular debris and cell conjugates for sorting.
- B.** NIH3T3 cells were trasduced with two retroviruses: one expressing ICOS from either huIcos^{F1} or huIcos^{F3}, the other expressing Roquin^{WT}. Two cell populations were sorted separately: one cell population expressing high level of Roquin (GFP^{High}); the other cell population lacking Roquin expression (GFP^{Nil}). The purity of the sorted cells was measured. Total RNA was isolated and quantitative RT-PCR was performed to measure *HuCD4* mRNA levels, which were normalized to β -actin. The bar graph shows relative huCD4 mRNA in GFP^{High} cells compared to GFP^{Nil} cells (GFP^{Hi}/GFP^{NiL} ratio).

The filled bar represents huIcos^{F1} and the open bar represents huIcos^{F3}. Data shown represent mean values \pm S.D. with n=4 different primer pairs designed to amplify different fragments of huCD4 cDNA.

This experiment was preformed by DI Yu and Xin Hu.

effect acts through the control of mRNA decay, or some effect might be attributed to Roquin's action on translation of mRNA. Since Roquin's repression of huCD4 (protein) expression is reduced to 70%-80% of the levels seen in empty vector controls (figure 4.4), and this exactly corresponds to the levels of repression of target mRNA levels described above, it is likely that of Roquin's repressive effect acts at the level of regulation of mRNA abundance (see also below for further evidence showing Roquin regulates mRNA decay).

4.5 SUMMARY

The results in this chapter have demonstrated that the most distal fragment within *Icos* 3'UTR mRNA - *Icos-3'UTR-F3*- is both necessary and sufficient to mediate ICOS repression by Roquin. We have shown further evidence that Roquin represses ICOS expression in a dose-dependent manner. Importantly, and as shown in the previous chapter Roquin^{M199R} is a less efficient repressor of huICOS and huCD4 expression irrespective of the level of Roquin expression, suggesting once again that the *sanroque* mutation reduces but does not abolish this repressive activity of Roquin. Finally, I have provided evidence that Roquin's effects are likely to regulate mRNA abundance as opposed to regulation of translation.

Subsequent to my experiments described above identifying the region of *Icos* 3'UTR important for Roquin's repressive effect, and pin-pointing the latter as an effect of mRNA stability, Di Yu, a PhD student in the lab performed *in silico* analysis of this F3 region within ICOS 3'UTR, and identified the existence of five miRNA-binding sites within this stretch of RNA. Importantly, this mRNA segment lacked typical AU-rich elements. Di Yu and I together, subcloned the three minimal 47bp regions; two of them containing the microRNA-binding sites and discovered only one of these minimal 47bp regions could mediate ICOS repression by Roquin. Intriguingly, this region alone contained four of the five miRNA-binding sites, and one of these, *hsa miR-101*, has been found to be expressed in both NIH3T3 cells and mouse T cells. When Di Yu inverted two nucleotides of ICOS 3'UTR mRNA complementary to seed sequence of this miRNA predicted to abolish binding of the miRNA, the repressive activity was severely impaired. This suggests ICOS repression by Roquin might involve the miRNA machinery (Yu *et al.*, 2007).

In parallel, our collaborators Andy Hee-Meng Tan and Kong Peng Lam confirmed Roquin's effect on *Icos* mRNA abundance was in fact due to increasing mRNA decay. This was performed activating mouse EL4 cells before transfection with Roquin followed by treatment with Actinomycin D (ActD) to block transcription. They showed that in ActD-treated cells, Roquin overexpression shortened *Icos* mRNA half-life by half compared to empty vector.

§ FIVE §

TNF is also a target for post-transcriptional regulation by Roquin

5. 1 Introduction

The chronic course of most autoimmune diseases including autoimmune arthritis, Systemic Lupus Erythematosus and inflammatory bowel disease, has been shown to at least in part be the consequence of a sustained inflammatory process due to the inability to turn off pro-inflammatory signals – including cytokines - produced by innate immune cells (Nathan, 2002). Amongst innate cells of the immune system, macrophages, neutrophils and mast cells play prominent roles in many inflammatory conditions.

Multiple signals are capable of inducing macrophage activation either by surface receptor ligation, as is the case of ligands for Toll-like receptors (TLR) and immunoglobulins that bind Fc receptors, or simply by crossing the cellular membrane as is the case of nitric oxide (NO) and PMA (Han and Ulevitch, 2005; Mandik-Nayak and Allen, 2005). Regardless of the stimuli, macrophage stimulation results in the generation of downstream signals that converge to promote transcription exerted by NFκB and MAPK pathways, resulting in changes in gene expression (Han and Ulevitch, 2005). TNF is one of the key target genes of NFκB and an important mediator of pro-inflammatory responses.

TNF is a cytokine involved in systemic inflammation and causes apoptotic cell death, cellular proliferation, and cell differentiation (Locksley *et al.*, 2001). TNF also plays a role in immune regulation and lymphoid organogenesis (Douni *et al.*, 1995; Pfeffer, 2003). Recent studies have identified a role for TNF in several autoimmune diseases in humans and mouse models including lupus, autoimmune diabetes and autoimmune arthritis (Chamberlain *et al.*, 2006; Conway *et al.*, 2001; Kassiotis and Kollias, 2001; Nash and Florin, 2005). Anti-TNF therapy has also shown dramatic success in the symptomatic treatment of patients with rheumatoid arthritis.

Sanroque mice have high levels of serum TNF compared to littermate controls (D. Silva personal communication). In a model of arthritis induced by transfer of K/BxN arthritogenic serum into lymphocyte-deficient RAG1^{-/-} mice, arthritis is more severe when the recipient mice are homozygous for the *sanroque* mutation (D. Silva *et al.*, manuscript in preparation). The cytokines IL-1β and TNF have been shown to be important effectors of the antibody-mediated arthritis of K/BxN mice (Ji *et al.*, 2002). Increased severity of arthritis in *sanroque* RAG1^{-/-} mice has been shown to be

associated with increased amounts of TNF produced by *sanroque* macrophages compared to controls. When the levels of *Tnf* mRNA were assessed by real time PCR, *sanroque* macrophages were shown to have higher levels of *Tnf* mRNA compared to Roquin+/+ macrophages (D. Silva personal communication).

TNF expression is not only regulated at the transcriptional level, but there is also solid evidence that it is also post-transcriptionally regulated. TNF induces the expression of tristetraprolin (TTP), which in turn destabilizes and degrades *Tnf* mRNA. Importantly, TTP knockout (KO) mice develop a systemic inflammatory syndrome with severe polyarthritis and autoimmunity, as well as medullary and extramedullary myeloid hyperplasia (Carballo *et al.*, 1998; Carrick *et al.*, 2004; Taylor *et al.*, 1996). TTP^{KO} macrophages, derived from fetal liver, bone marrow and peritoneal cavity, released more TNF than macrophages from their TTP^{WT} littermates (Carballo *et al.*, 1998). All of these phenotypes were associated with an increase in the stability of TNF in the KO cells. In experiments blocking TNF transcription with Actinomycin D, in the absence of TTP there was an increase in the half-life of TNF, implying a decrease in *Tnf* mRNA turnover rate (Blackshear, 2002). The molecular mechanism of the regulation exerted by TTP has been elucidated: TTP, which contains two tandem CCCH domains – nearly identical to Roquin’s single CCCH domain, directly binds a highly rich AU-rich region within *Tnf* 3’UTR mRNA (Fig. 5.1) and in doing so enhances deadenylation which leads to mRNA decay (Carballo *et al.*, 1998).

If we combine the evidence that there is dysregulation of TNF expression in *sanroque* mice demonstrated by very high *Tnf* mRNA levels and serum TNF, together with our knowledge of Roquin regulating other targets (*Icos*) at the mRNA level in stress granules, and the data showing TNF is strongly regulated at the level of mRNA stability, we can put forward the hypothesis that Roquin participates in TNF’s post-transcriptional regulation. We then set out to test whether Roquin’s putative role in TNF’s regulation acts on *Tnf* 3’UTR.

5.2 Roquin regulates TNF expression through its 3'UTR

To test the hypothesis that *Tnf* 3'UTR mRNA is required for Roquin's repression of TNF expression, I used the retroviral transduction assay described in the previous chapter, generating the construct *Tnf*^{3'UTR}. To do this, cDNA from the 3'UTR fragment of *Tnf mRNA*, excluding the coding region, was subcloned into the multiple cloning site upstream of the IRES in the retroviral vector pR-IRES-huCD4 (Figure 5.2).

A retroviral supernatant from this retroviral construct was harvested from Phoenix cell cultures and titrated as described in the previous chapter to achieve 50%-60% transduction. NIH3T3 cells were then co-transduced with retroviruses containing supernatants from:

- Either pR-Roquin^{WT}-IRES-GFP or pR-Roquin^{M199R}-IRES-GFP or pR-IRES-GFP empty vector
- plus*
- pR-*Tnf*^{3'UTR}-IRES-huCD4

Two days after transduction, NIH3T3 cells were analysed by flow cytometry. The gating strategy used for this analysis is shown in Figure 5.3. GFP versus huCD4 fluorescence was plotted to separately gate three different populations according to the level of GFP expression (GFP^{Hi}, GFP^{Low} and GFP^{NIL}) for each of the three GFP vectors (Roquin^{WT}, Roquin^{M199R}, or empty vector).

I quantified the level of TNF repression by the different Roquin vectors as the percentage of huCD4 level seen in cells transduced with the empty pR-IRES-GFP construct.

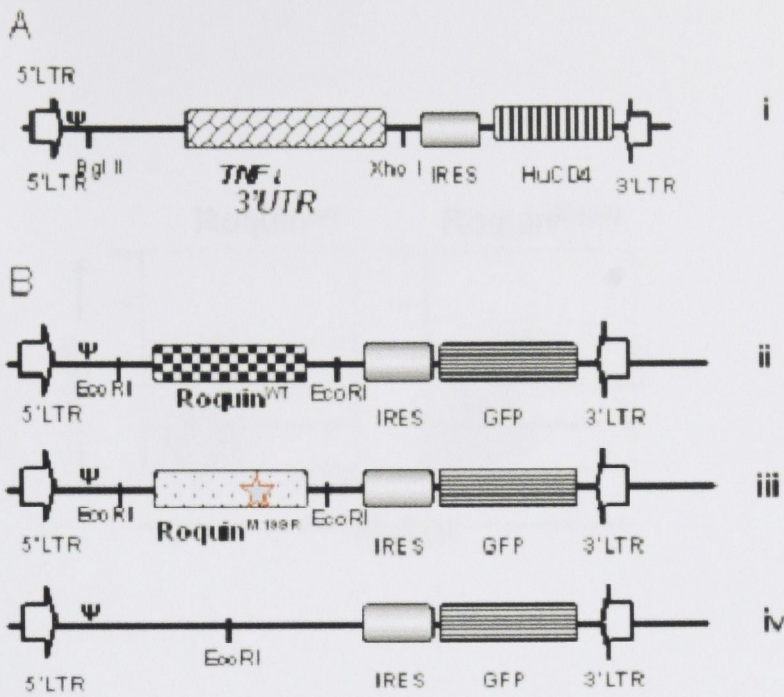


Figure 5.2 Schematic representations of the retroviral constructs.

A. The 3'UTR of *Tnf* was inserted into the retroviral pR-IRES-huCD4 using the restriction enzymes BglIII and XhoI.

pR-*Tnf*^{3'UTR}-IRES-huCD4

B. Wild-type (Roquin^{WT}) and mutant (Roquin^{M199R}) Roquin cDNA were inserted into the retroviral vector pR-IRES-GFP using the restriction enzyme EcoR I.

(ii) pR-Roquin^{WT}-IRES-GFP

(iii) pR-Roquin^{M199R}-IRES-GFP

(iv) pR-IRES-GFP (empty vector control)

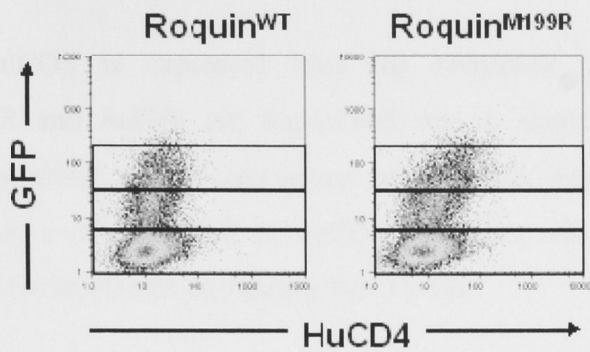


Figure 5.3

Flow cytometric analysis of NIH3T3 cells transduced with TNF 3'UTR and either Roquin^{WT} (left) or Roquin^{M199R} (right).

Dot-plots show GFP (Roquin) vs huCD4 (reporter of *Tnf* 3'UTR) expression. The rectangular gates indicate GFP^{high}, GFP^{low} and GFP^{Nil} populations (from top to bottom respectively) used to quantify Roquin's effect.

5.3 Roquin^{M199R} causes an increase in *Tnf* 3'UTR-containing transcripts.

Since huICOS is expressed from the bicistronic pR-IRES-huCD4 vector both *Tnf* 3'UTR and *huCd4* are transcribed into a single transcript. Therefore, if the regulatory effect is a consequence of Roquin's regulation of *Tnf* 3'UTR mRNA abundance, a parallel shift in huCD4 expression should be observed in cells co-transduced with vectors containing *Tnf* 3'UTR.

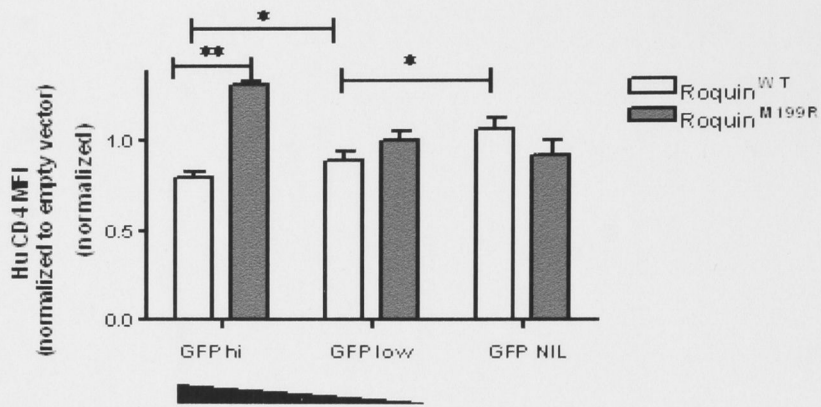
HuCD4 expression was measured by flow cytometry. As observed in the case of Icos, Roquin^{WT} repressed huCD4 expression from transcripts containing *Tnf* 3'UTR. Nevertheless, this repressive effect was smaller (1.5-fold reduction of huCD4 expression in GFP^{hi} cells compared with GFP^{NIL} cells, Figure 5.4A) than that observed for *huIcos* under the same experimental conditions (Figure 3.2: 8-fold reduction of ICOS expression and 4-fold reduction of huCD4 expression in GFP^{hi} cells compared to GFP^{NIL} cells). Strikingly, Roquin^{M199R} showed a potent enhancement of huCD4 expression in GFP^{hi} cells, to 130% of levels seen in GFP^{NIL} cells. Again, this effect contrasts with that seen for *huIcos*, in which Roquin^{M199R} also repressed expression, albeit less potently than Roquin^{WT}.

This experiment was carried out in triplicate and repeated twice (also in triplicate) to make sure the results were reproducible. In one of the two repeat experiments (experiment 2), there was no obvious repression exerted by Roquin^{WT}, highlighting the fact that the repression seen in A and C is subtle. Again, in both repeat experiments, transduction with Roquin^{M199R} constructs had a profound effect, increasing significantly the expression of huCD4 in GFP^{hi} cells to 160% of the levels found in GFP^{NIL} cells (Figure 5.4 GFP^{hi}).

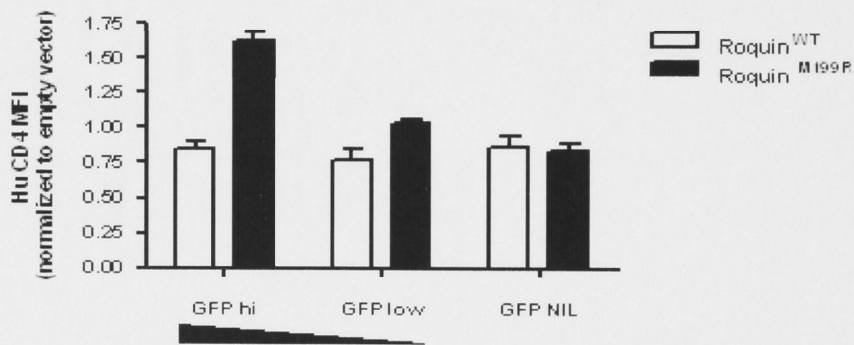
The results shown in both of these experiments differ from those obtained for Roquin's regulation of ICOS expression, in which both Roquin^{WT} and Roquin^{M199R} exerted a repressive effect on *Icos* 3'UTR, although Roquin^{M199R} was a less potent repressor. It thus appears Roquin^{M199R} acts in a dominant negative fashion to increase (probably stabilize) *Tnf* 3'UTR mRNA.

Fig. 5.4

A. Experiment 1



B. Experiment 2



C. Experiment 3

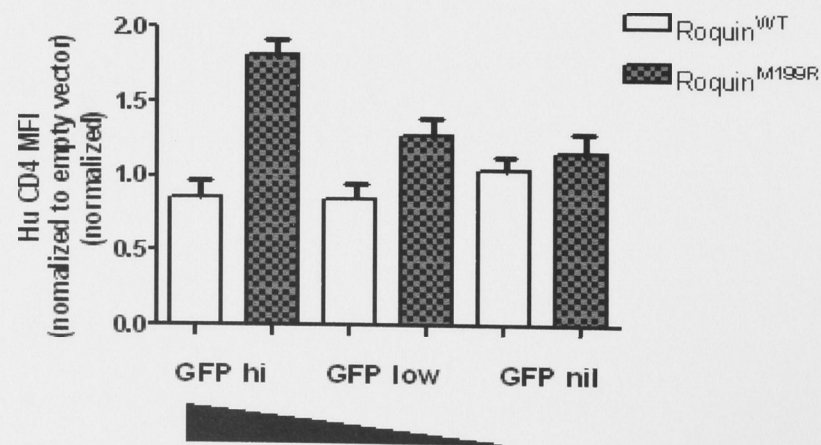


Figure 5.4 Regulation of TNF expression by Roquin.

NIH3T3 cells were transduced by two retroviruses: one expressing $Tnf^{3'UTR}$; the other expressing either Roquin^{WT}, Roquin^{M199R} or an empty vector control.

The regulation of TNF expression (as assessed by measuring MFI of the reporter huCD4) by Roquin^{WT} and Roquin^{M199R} were compared using the same quantification method as described for the regulation of *Icos* in chapter 4.

Open bars represent cells transduced with RoquinWT and filled bars represent cells transduced with RoquinM199R. Data shown represent mean values \pm S.D with n=3. Student's test *P<0.05; **P<0.01.

A, B and C show results for three separate experiments using the same vectors, but different batches of retroviruses. In experiments 1 and 3, but not in experiment 2, Roquin^{WT} appears to exert a mild suppressor effect.

Tentative explanations for the discordance between Roquin's regulatory effects on ICOS and TNF are provided in the discussion chapter.

5.4 Roquin^{M199R} increases *Tnf* 3'UTR transcripts in a gene-dose dependent manner

We also observed a gene-dose effect for Roquin's regulatory actions on *Tnf* 3'UTR. Compared to the 160% levels of huCD4 expression in cells transduced with high levels of Roquin^{M199R} (GFP^{hi}) compared to GFP^{NIL} cells, cells transduced with low levels of Roquin^{M199R} (GFP^{low}) had only a very modest increase in huCD4 ($p < 0.01$). HuCD4 levels in GFP^{low} cells were only slightly higher ($p < 0.05$) than those of cells not transduced with Roquin^{M199R} (Roquin^{NIL}).

5.5 The 3'UTR of *Tnf* mRNA contains AREs and microRNA target sequences

It is well known that the AU-rich elements (AREs) are important regulators of *Tnf* mRNA stability and control TNF-alpha biosynthesis (Hel *et al.*, 1996; Jacob *et al.*, 1996).

In the previous chapter I mentioned that ICOS regulation by Roquin appears not to depend on AREs, but on conserved miRNA target sites. In order to identify putative miRNA target sites within the 3'UTR of *Tnf* mRNA, I used the software MiRanda for predicting miRNA target sequences. As illustrated in Figure 5.5. I found that the 3'UTR of *Tnf* mRNA contains not only the well-known AREs (in yellow) but also several microRNA-target sites, including mmu-miR-149, mmu-miR-130a and mmu-miR-130b (Figure 5.5). These miRNAs have been reported to be expressed in myeloid cells (Monticelli *et al.*, 2005).

5.6 Summary

In this chapter, I used retrovirus-mediated transduction of NIH3T3 cells to test whether the 3'UTR *Tnf* mRNA can be regulated by Roquin and thus explain at the molecular level the increased levels of *Tnf* mRNA found in activated *sanroque* macrophages.

I have demonstrated that while Roquin^{WT} might exert a very mild repressive effect Roquin^{M199R} induces a striking increase in expression of mRNA expressed from a transcript containing *Tnf* 3'UTR mRNA. This suggests Roquin might act in a dominant negative fashion to regulate some of its targets.

These results demonstrate TNF is also a target for Roquin's post-transcriptional regulation, and this regulation requires the 3'UTR sequence. Since huCD4 is translated separately from the upstream transcript, the regulation observed is likely to occur at the level of mRNA abundance as opposed to regulation of translation. Further experiments blocking transcription with Actinomycin D and quantifying mRNA decay in double transduced cells are underway to confirm Roquin specifically regulates *Tnf* mRNA stability.

Using bioinformatic tools we found that the 3'UTR of *Tnf* mRNA contains several miRNA target binding sequences that are very conserved between human and mouse. We speculate Roquin might regulate *Tnf* mRNA stability acting through one or several of these miRNA-target sites.

§ SIX §

General discussion

6.1 Limiting ICOS expression emerges as a novel mechanism to maintain immune tolerance

A two-signal model of T cell activation has been used to explain how to prevent self-reactive T cells that make it to the periphery from being activated, and thus maintaining T cell tolerance (Goodnow *et al.*, 2005; Lafferty *et al.*, 1980; Matzinger, 1994). According to this model, in addition to a signal through the T cell receptor (TCR) after binding its specific peptide forming a complex with MHC molecules, a second signal, named the co-stimulatory signal, is necessary for T cell activation and differentiation into an effector cell (Tafari *et al.*, 2001). Co-stimulation mainly occurs through ligation of CD28 (Harding *et al.*, 1992). Although CD28 is constitutively expressed on T cells, its ligands B7.1 and B7.2 are generally only induced on antigen presenting cells (APCs), after exposure to foreign antigens (Carreno and Collins, 2002; Greenwald *et al.*, 2005; Nabavi *et al.*, 1992). Therefore, self-reactive T cells are unlikely to receive the co-stimulation from CD28 since APCs exposed to self-antigens do not upregulate B7 molecules (Sharpe and Freeman, 2002) and M. Linterman (personal communication).

It is paradoxical that while restricted co-stimulation through the CD28-B7s axis relies on the inducibility of B7 molecules on APCs, such restriction does not apply through the ICOS-ICOSL pathway. This is because, unlike CD28 ligands, ICOS ligand (ICOSL or B7h) is constitutively expressed on most APCs, including dendritic cells and B cells (Ling *et al.*, 2000; Yoshinaga *et al.*, 1999). In this situation, limiting the level of ICOS expression on naïve T cells emerges as a crucial checkpoint to maintain T cell tolerance (Yu *et al.*, 2007). To my knowledge, no mechanisms besides the one proposed in this study have been described that operate to limit the expression of ICOS on T cells.

There have been studies showing ICOS expression can be increased by transcriptional regulation, after combined stimulation through TCR and CD28 (Tan *et al.*, 2006). It is assumed that, naïve CD44^{Low} CD4⁺ T cells have not received activation signals through TCR/CD28; it is only after these signals are received that T cells make the transition to become activated / effector CD44^{high} T cells. However, *sanroque* naïve T cells already express significantly high levels of ICOS (Vinuesa *et al.*, 2005a), suggesting ICOS overexpression is not solely driven by transcriptional regulation.

My work and that of Di Yu has demonstrated that a novel mechanism regulating the degradation of basal level of ICOS transcripts is impaired in the presence of defective Roquin function. This results in aberrant overexpression of ICOS on naïve T cells that might be sufficient to provide co-stimulation to self-reactive T cells that bind autoantigens, resulting in a break of T cell anergy and leading to autoimmune pathology.

Since my experimental work concluded, Di Yu has demonstrated that halving the levels of ICOS on *sanroque* mice by generating *Roquin^{san/san}:Icos^{+/-}* mice (i.e. heterozygous for an *Icos* null allele) reduces the lymphadenopathy, splenomegaly, and T and B cell accumulation in the same proportion, although there is only a subtle reduction in T_{FH} cell numbers, germinal centres and autoantibodies (Yu *et al.*, 2007). These mice still express twice the levels of *Icos* than *Roquin^{WT}* wild type mice. It will be important to see whether *Icos* deficiency in *Roquin^{san/san}:icos^{-/-}* mice (currently being generated) can fully correct the lupus phenotype, or other T_{FH} molecules that are also found overexpressed in *sanroque* mice such as IL-21 also contribute to the pathology.

This theory of why ICOS overexpression on naïve cells bypasses the requirement for CD28 co-stimulation and breaks tolerance could be formally tested by crossing *sanroque* mice to CD28 knockout mice. If this hypothesis is correct, a substantial amount of the *sanroque* pathology should still be obvious in mice lacking CD28. Indeed, these experiments are underway in my laboratory, and initial results suggest ICOS overexpression does overcome the need for CD28 co-stimulation during different phases of CD4⁺ immune responses (M. Linterman, personal communication). It will be interesting to see whether *sanroque*: CD28^{-/-} mice still develop the lupus-like syndrome.

Another explanation for the ICOS-driven break in tolerance may be its effects on T_{FH} cell homeostasis. ICOS signaling has been shown to be necessary for the development and maintenance of T_{FH} cells and germinal centres (Akiba *et al.*, 2005; Warnatz *et al.*, 2006). Thus, it is also possible that autoimmunity in *sanroque* mice is simply a consequence of enhancement of T_{FH} generation and accumulation, due to *Roquin^{M199R}*-driven ICOS overexpression. There is substantial evidence to show T_{FH} cells have the highest levels of ICOS expression (Hutloff *et al.*, 1999), and these cells are very potent helpers of germinal centre B cells (Dong and Nurieva, 2003). The excessive number of T_{FH} cells and spontaneous germinal center formation seen in *sanroque* mice support this possibility.

The two possibilities mentioned above are not mutually exclusive; in fact they are related to each other. For instance, both mechanisms contribute towards the generation of self-reactive T_{FH} cells, and thus both would help self-reactive germinal center B cells produce pathological high affinity autoantibodies.

This novel checkpoint in T cell tolerance revealed by our research expands our understanding of the regulation of co-stimulation to maintain tolerance and suggests partial antagonism of ICOS signaling might prove a good therapeutic strategy for lupus patients with dysregulated T_{FH} function.

6.2 The role of Roquin in promoting *Icos* mRNA decay

We have demonstrated Roquin represses ICOS expression through *Icos* 3'UTR mRNA (Figure 3.10). It is the most distal fragment, F3, within the 3'UTR that plays an essential role in mediating this repression (Figure 4.1). Importantly, my experiments show that this repression reduces mRNA abundance (Figure 4.5). However, with this experiment alone we cannot unequivocally conclude that this effect is a consequence of accelerating *Icos* mRNA decay. In comparison with other fragments, for example F1, only F3 was capable of mediating Roquin's repression on mRNA abundance. Since the cDNAs for F1 and F3 are separately subcloned into the multiple cloning site before the internal ribosomal entry site (IERS) it is possible that the F3 sequence, but not the F1 sequence, may affect the murine stem cell virus (MSCV) promoter and inhibit transcription of *huCd4* mRNA, thus reducing *huCd4* mRNA levels measured by qRT-PCR. Nevertheless this would be extremely unlikely. Fortunately, our collaborator Andy Tan (from Kong Peng Lam's laboratory, Singapore) has performed the experiment that proves the increased levels of mRNA are a consequence of Roquin's effects on mRNA decay. He has been able to show that Roquin overexpression in EL4 cells (a T cell line) accelerates *Icos* mRNA decay, by measuring the half-life of endogenous *Icos* mRNA after inhibition of transcription with Actinomycin D (Yu *et al.*, 2007). Our combined data show that Roquin limits *Icos* mRNA by enhancing mRNA decay through the F3 segment within its' 3'UTR.

6.3 The M199R mutation in Roquin impairs but does not abolish ICOS repression

The experiments performed in this thesis show the M199R mutation in Roquin impairs its ability to repress ICOS expression (Figure 3.10). Nevertheless, the effects are mild. *A priori*, I would have expected to see a more dramatic effect, since it is this mutation that leads to the very dramatic overexpression of ICOS in *sanroque* mice. At least two different arguments may explain this discrepancy. First, in the original published experiments, it was clearly shown that overexpression of the M199R allele into *sanroque* T cells partially corrected the ICOS^{high} phenotype, suggesting this allele had residual suppressive function, and could act in a manner comparable to Roquin, albeit with reduced efficiency when overexpressed. This is what is called a hypomorphic allele, as opposed to a loss of function allele. Second, the NIH3T3 cells used in these experiments have endogenous Roquin expression since Roquin is expressed ubiquitously. Thus, it is possible that wild type endogenous Roquin might still exert a suppressive effect on ICOS expression that cannot be fully inhibited by overexpression of mutant Roquin. Ideally, these experiments should be performed in Roquin knockout cells.

The M199R mutation lies in the novel ROQ domain of the Roquin protein (Vinuesa *et al.*, 2005a). The ROQ domain is essential to direct Roquin's localization to stress granules (V. Athanasopoulos, personal communication). Furthermore, a truncated form of Roquin lacking the ROQ domain completely loses the ability to repress ICOS expression (V. Athanasopoulos, personal communication). Together, these data suggest that localization of Roquin to SGs is crucial for Roquin's repression of ICOS expression.

6.4 How does Roquin regulate mRNA decay?

In SGs, translationally-arrested mRNAs are sorted so that they are routed either for degradation through the regulation of their stability or translation, or for re-initiation of translation (Anderson and Kedersha, 2006). Most proteins localizing to SGs such as eIF2/3/4E and HuR and TTP, have functions related to the regulation of translational

control and mRNA decay (Anderson and Kedersha, 2006). So the key question is how does Roquin act in SGs to promote *Icos* mRNA decay? There are several possibilities:

Since Roquin has a CCCH zinc finger domain found in many RNA binding proteins, the simplest model would predict that Roquin specifically binds to *Icos* mRNA thereby recruiting it to SGs. This would prevent translation, which normally occurs in the cytoplasm. Once Roquin has bound *Icos* mRNA, it would enhance its decay, possibly recruiting the miRNA machinery. An important part of the puzzle we have not solved is determining whether Roquin can directly bind *Icos* mRNA (or any mRNA). To sort this out, we can use the supershift assay that is commonly used for analyzing specific protein-nuclear acid binding interactions.

Another possibility is that the CCCH zinc finger domain simply aids Roquin to bind to RNA components in SG, and in doing so perhaps facilitate its recruitment to SGs, but does not specifically bind *Icos* mRNA. Once in SGs, Roquin may activate or enhance the machinery leading to *Icos* mRNA decay or direct *Icos* mRNA to P-bodies for further degradation. In order to prove this possibility, we would need some evidence to show that Roquin may bind non-specifically to different mRNAs and that *Icos* mRNA localizes to SGs independently of Roquin. The fact that Roquin also regulates *mf* mRNA, supports the idea Roquin might regulate many different short-lived mRNAs. If this is true, it is highly unlikely Roquin can specifically bind to all its targets, and thus an indirect mechanism like the one proposed here would be favored.

Another crucial question is whether the predicted E3 ubiquitin ligase activity of Roquin is required for ICOS repression. Roquin has a RING1 zinc-finger domain, which is found in many proteins with E3 ubiquitin ligase activity (Klug, 1999) and the Roquin homologue in *C. elegans*, RLE1, has been shown to have ubiquitin ligase activity (Li *et al.*, 2007). Thus, we cannot exclude the possibility that Roquin regulates *Icos* mRNA by aiding ubiquitylation (and thus degradation) of proteins that would normally stabilize mRNA. In this way, Roquin deficiency would lead to accumulation of mRNA stabilizing proteins, and thus an increase in certain mRNAs, including that of *Icos*. Interestingly, the mRNA stabilizing protein HuR has been reported to function in a ubiquitin / proteasome-dependent manner and it also localizes to SGs (Gallouzi *et al.*, 2000; Kedersha and Anderson, 2002; Laroia *et al.*, 2002). Therefore, it is possible that Roquin mediates ubiquitylation followed by degradation of HuR and in doing so it

accelerates mRNA decay of HuR targets (which may include *Icos* mRNA). This could be tested by investigating the repression of ICOS by Roquin in the presence of a proteasome inhibitor. A different way to answer this question would be by investigating whether a mutant version of Roquin that has lost the E3 ligase activity can regulate ICOS expression. Replacing the first cysteine in the RING domain with an alanine has been shown to abolish Cbl's E3 ligase activity; this same mutation could be introduced in Roquin to test this hypothesis.

6.5 A potential role for miRNAs in the regulation of *Icos* mRNA

There are several kinds of regulatory *cis*-acting elements in mRNAs that can mediate mRNA decay. AU-rich elements (AREs) have been identified in a large number of mRNAs and have been shown to be potent regulators of mRNA stability (Khabar, 2005). However, there is no typical ARE motif ("AUUUA" sequence) within F3 of human *Icos* mRNA 3'UTR. Recently, miRNA target sequences within mRNAs are emerging as an important group of *cis*-acting elements regulating mRNA translation and decay (Barreau *et al.*, 2005; Jackson and Standart, 2007). Using *in silico* analysis, Di Yu found several miRNA target sequences within the F3 region of *Icos* 3'UTR, including a region complementary to miRNA-101 target sequence. This miRNA had been found to be expressed in T cells (Monticelli *et al.*, 2005). Introduction of a mutation in the *Icos* mRNA sequence complementary to the seed region (predicted to abolish miRNA binding) impaired Roquin's ability to repress ICOS expression, strongly suggesting miRNAs are important for Roquin's effects on ICOS expression (Yu *et al.*, 2007).

6.6 TNF and other putative targets of Roquin's regulation

The other important finding in this thesis is the identification of *Tnf* as another target for Roquin's regulation. My data shows TNF is also regulated by Roquin post-transcriptionally. This is demonstrated by the experiment showing the 3'UTR of *Tnf* mRNA can mediate Roquin's regulation of the reporter huCD4.

There are two striking differences between Roquin's effects on *Icos* and *Tnf* mRNA:

1) While Roquin^{WT} exerts a potent suppressor effect on *Icos* mRNA, this is not so obvious in the case of *Tnf* mRNA. In fact repression was only apparent in the first of 3

experiments performed (Figure 5.4). In experiment 2, there was no statistically significant repression of *tnf* 3'UTR by Roquin.

2) By contrast, while Roquin^{M199R} shows only a mild reduction in the repressive action of Roquin on *Icos* mRNA, it exerts a very potent effect upon *Tnf* mRNA, increasing the expression of the reporter huCD4 considerably (Figure 5.4). It appears as if Roquin^{M199R} could be acting in a dominant negative way, i.e. the mutation in the overexpressed construct might be impairing the activity of endogenous wild type Roquin (which is maintaining the basal levels of TNF).

A possible explanation for this is that Roquin may regulate *Icos* mRNA and *Tnf* mRNA through slightly different mechanisms. *Tnf* mRNA has been shown to be regulated by TTP, through binding of typical AREs in its 3'UTR (Blackshear, 2002). Therefore, it would be important to establish whether Roquin's regulation of *Tnf* mRNA also occurs through AREs. If it is true that *Icos* mRNA is regulated by the miRNA machinery as speculated above, it is possible that the M199R mutation in Roquin affects in different ways microRNA regulation vs classical ARE-mediated mRNA decay.

The fact that Roquin regulates two different mRNAs post-transcriptionally, suggests that Roquin could have more targets. In the microarray experiments performed in our laboratory, most genes that showed increased mRNA levels in CD4⁺ T cells from *sanroque* mice (compared to wild-type littermates) are those genes classified as having short half-lives (Vinuesa *et al.*, 2005a). It is then possible that all these short-lived mRNAs found in CD4⁺T cells (perhaps only during a particular maturation / activation / differentiation stage) are regulated by Roquin.

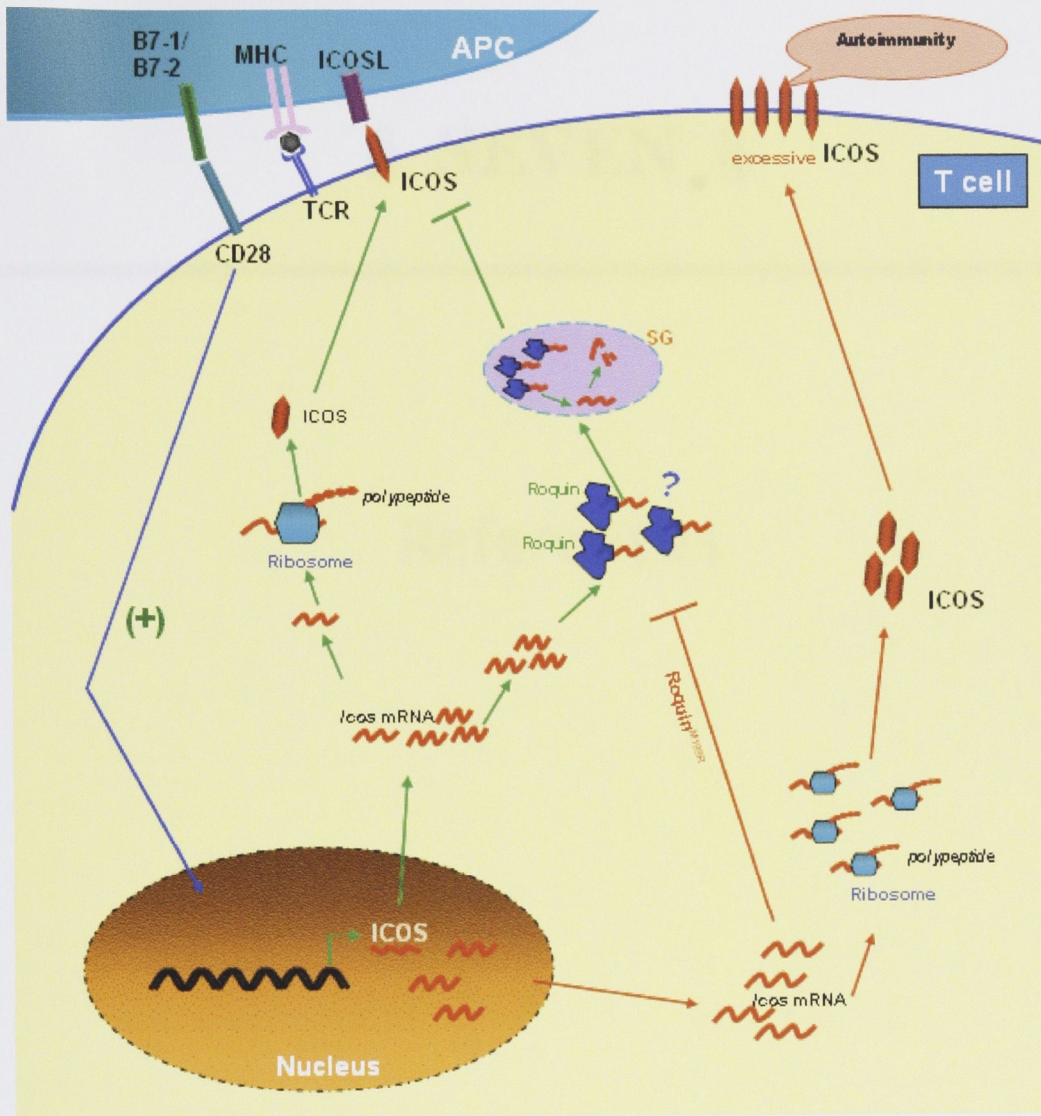


Fig. 6.7. Model of how Roquin regulates *Icos* expression

In wild type T cells *Icos* transcription is induced by TCR and CD28 signaling; some *Icos* transcripts encounter Roquin in the cytoplasm or in SGs; Roquin then promotes the degradation of *Icos* transcripts; other *Icos* transcripts are translated to be expressed on the surface of T cells, where ICOS protein interacts with ICOSL to mediate costimulation signaling for T cell activation and differentiation.

In *sanroque* T cells: the Roquin-mediated *Icos* mRNA decay is impaired by the mutation in Roquin so that there is much more ICOS expressed on the surface of T cells; unlimited ICOS expression breaks tolerance by activating self-reactive T cells, hyperactivating T cells or exaggerating aberrant differentiation.

§ SEVEN §

References

- Abbas, A.K., J. Lohr, B. Knoechel, and V. Nagabhushanam. 2004. T cell tolerance and autoimmunity. *Autoimmun Rev.* 3:471-5.
- Akbari, O., G.J. Freeman, E.H. Meyer, E.A. Greenfield, T.T. Chang, A.H. Sharpe, G. Berry, R.H. DeKruyff, and D.T. Umetsu. 2002. Antigen-specific regulatory T cells develop via the ICOS-ICOS-ligand pathway and inhibit allergen-induced airway hyperreactivity. *Nat Med.* 8:1024-32.
- Akiba, H., K. Takeda, Y. Kojima, Y. Usui, N. Harada, T. Yamazaki, J. Ma, K. Tezuka, H. Yagita, and K. Okumura. 2005. The role of ICOS in the CXCR5+ follicular B helper T cell maintenance in vivo. *J Immunol.* 175:2340-8.
- Anderson, P., and N. Kedersha. 2006. RNA granules. *J Cell Biol.* 172:803-8.
- Ansel, K.M., I. Djuretic, B. Tanasa, and A. Rao. 2006. Regulation of Th2 differentiation and Il4 locus accessibility. *Annu Rev Immunol.* 24:607-56.
- Bachmaier, K., C. Krawczyk, I. Kozieradzki, Y.Y. Kong, T. Sasaki, A. Oliveira-dos-Santos, S. Mariathasan, D. Bouchard, A. Wakeham, A. Itie, J. Le, P.S. Ohashi, I. Sarosi, H. Nishina, S. Lipkowitz, and J.M. Penninger. 2000. Negative regulation of lymphocyte activation and autoimmunity by the molecular adaptor Cbl-b. *Nature.* 403:211-6.
- Barreau, C., L. Paillard, and H.B. Osborne. 2005. AU-rich elements and associated factors: are there unifying principles? *Nucleic Acids Res.* 33:7138-50.
- Bartel, D.P. 2004. MicroRNAs: genomics, biogenesis, mechanism, and function. *Cell.* 116:281-97.
- Berezikov, E., and R.H. Plasterk. 2005. Camels and zebrafish, viruses and cancer: a microRNA update. *Hum Mol Genet.* 14 Spec No. 2:R183-90.
- Blackshear, P.J. 2002. Tristetraprolin and other CCCH tandem zinc-finger proteins in the regulation of mRNA turnover. *Biochem Soc Trans.* 30:945-52.
- Breitfeld, D., L. Ohl, E. Kremmer, J. Ellwart, F. Sallusto, M. Lipp, and R. Forster. 2000. Follicular B helper T cells express CXC chemokine receptor 5, localize to B cell follicles, and support immunoglobulin production. *J Exp Med.* 192:1545-52.
- Brooks, S.A., J.E. Connolly, and W.F. Rigby. 2004. The role of mRNA turnover in the regulation of tristetraprolin expression: evidence for an extracellular signal-regulated kinase-specific, AU-rich element-dependent, autoregulatory pathway. *J Immunol.* 172:7263-71.
- Carballo, E., W.S. Lai, and P.J. Blakeshear. 1998. Feedback inhibition of macrophage tumor necrosis factor-alpha production by tristetraprolin. *Science.* 281:1001-5.
- Carreno, B.M., and M. Collins. 2002. The B7 family of ligands and its receptors: new pathways for costimulation and inhibition of immune responses. *Annu Rev Immunol.* 20:29-53.
- Carrick, D.M., W.S. Lai, and P.J. Blakeshear. 2004. The tandem CCCH zinc finger protein tristetraprolin and its relevance to cytokine mRNA turnover and arthritis. *Arthritis Res Ther.* 6:248-64.
- Casciola-Rosen, L.A., G. Anhalt, and A. Rosen. 1994. Autoantigens targeted in systemic lupus erythematosus are clustered in two populations of surface structures on apoptotic keratinocytes. *J Exp Med.* 179:1317-30.
- Chamberlain, G., M. Wallberg, D. Rainbow, K. Hunter, L.S. Wicker, and E.A. Green. 2006. A 20-Mb region of chromosome 4 controls TNF-alpha-mediated CD8+ T cell aggression toward beta cells in type 1 diabetes. *J Immunol.* 177:5105-14.
- Chang, T.C., and J.T. Mendell. 2007. microRNAs in vertebrate physiology and human disease. *Annu Rev Genomics Hum Genet.* 8:215-39.
- Cheadle, C., J. Fan, Y.S. Cho-Chung, T. Werner, J. Ray, L. Do, M. Gorospe, and K.G. Becker. 2005. Control of gene expression during T cell activation: alternate regulation of mRNA transcription and mRNA stability. *BMC Genomics.* 6:75.
- Cher, D.J., and T.R. Mosmann. 1987. Two types of murine helper T cell clone. II. Delayed-type hypersensitivity is mediated by TH1 clones. *J Immunol.* 138:3688-94.
- Chtanova, T., S.G. Tangye, R. Newton, N. Frank, M.R. Hodge, M.S. Rolph, and C.R. Mackay. 2004. T follicular helper cells express a distinctive transcriptional profile, reflecting their role as non-Th1/Th2 effector cells that provide help for B cells. *J Immunol.* 173:68-78.
- Conne, B., A. Stutz, and J.D. Vassalli. 2000. The 3' untranslated region of messenger RNA: A molecular 'hotspot' for pathology? *Nat Med.* 6:637-41.
- Conway, J.G., R.C. Andrews, B. Beaudet, D.M. Bickett, V. Boncek, T.A. Brodie, R.L. Clark, R.C. Crumrine, M.A. Leenitzer, D.L. McDougald, B. Han, K. Hedeem, P. Lin, M. Milla, M. Moss, H. Pink, M.H. Rabinowitz, T. Tippin, P.W. Scates, J. Selph, S.A. Stimpson, J. Warner, and J.D. Becherer. 2001. Inhibition of tumor necrosis factor-alpha (TNF-alpha) production and arthritis in the rat by GW3333, a dual inhibitor of TNF-alpha-converting enzyme and matrix metalloproteinases. *J Pharmacol Exp Ther.* 298:900-8.
- Coyle, A.J., and J.C. Gutierrez-Ramos. 2004. The role of ICOS and other costimulatory molecules in allergy and asthma. *Springer Semin Immunopathol.* 25:349-59.

- Diamond, B., and M.D. Scharff. 1984. Somatic mutation of the T15 heavy chain gives rise to an antibody with autoantibody specificity. *Proc Natl Acad Sci U S A*. 81:5841-4.
- Dong, C., A.E. Juedes, U.A. Temann, S. Shresta, J.P. Allison, N.H. Ruddle, and R.A. Flavell. 2001a. ICOS co-stimulatory receptor is essential for T-cell activation and function. *Nature*. 409:97-101.
- Dong, C., and R.I. Nurieva. 2003. Regulation of immune and autoimmune responses by ICOS. *J Autoimmun*. 21:255-60.
- Dong, C., U.A. Temann, and R.A. Flavell. 2001b. Cutting edge: critical role of inducible costimulator in germinal center reactions. *J Immunol*. 166:3659-62.
- Douni, E., K. Akassoglou, L. Alexopoulou, S. Georgopoulos, S. Haralambous, S. Hill, G. Kassiotis, D. Kontoyiannis, M. Pasparakis, D. Plows, L. Probert, and G. Kollias. 1995. Transgenic and knockout analyses of the role of TNF in immune regulation and disease pathogenesis. *J Inflamm*. 47:27-38.
- Fan, J., X. Yang, W. Wang, W.H. Wood, 3rd, K.G. Becker, and M. Gorospe. 2002. Global analysis of stress-regulated mRNA turnover by using cDNA arrays. *Proc Natl Acad Sci U S A*. 99:10611-6.
- Fang, S., K.L. Lorick, J.P. Jensen, and A.M. Weissman. 2003. RING finger ubiquitin protein ligases: implications for tumorigenesis, metastasis and for molecular targets in cancer. *Semin Cancer Biol*. 13:5-14.
- Furuzawa-Carballeda, J., M.I. Vargas-Rojas, and A.R. Cabral. 2007. Autoimmune inflammation from the Th17 perspective. *Autoimmun Rev*. 6:169-75.
- Gallouzi, I.E., C.M. Brennan, M.G. Stenberg, M.S. Swanson, A. Eversole, N. Maizels, and J.A. Steitz. 2000. HuR binding to cytoplasmic mRNA is perturbed by heat shock. *Proc Natl Acad Sci U S A*. 97:3073-8.
- Gingerich, T.J., J.J. Feige, and J. LaMarre. 2004. AU-rich elements and the control of gene expression through regulated mRNA stability. *Anim Health Res Rev*. 5:49-63.
- Goodnow, C.C., J. Sprent, B. Fazekas de St Groth, and C.G. Vinuesa. 2005. Cellular and genetic mechanisms of self tolerance and autoimmunity. *Nature*. 435:590-7.
- Graham, D.S., A.K. Wong, N.J. McHugh, J.C. Whittaker, and T.J. Vyse. 2006. Evidence for unique association signals in SLE at the CD28-CTLA4-ICOS locus in a family-based study. *Hum Mol Genet*. 15:3195-205.
- Greenwald, R.J., G.J. Freeman, and A.H. Sharpe. 2005. The B7 family revisited. *Annu Rev Immunol*. 23:515-48.
- Grimbacher, B., A. Hutloff, M. Schlesier, E. Glocker, K. Warnatz, R. Drager, H. Eibel, B. Fischer, A.A. Schaffer, H.W. Mages, R.A. Kroczeck, and H.H. Peter. 2003. Homozygous loss of ICOS is associated with adult-onset common variable immunodeficiency. *Nat Immunol*. 4:261-8.
- Han, J., and R.J. Ulevitch. 2005. Limiting inflammatory responses during activation of innate immunity. *Nat Immunol*. 6:1198-205.
- Harding, F.A., J.G. McArthur, J.A. Gross, D.H. Raulet, and J.P. Allison. 1992. CD28-mediated signalling co-stimulates murine T cells and prevents induction of anergy in T-cell clones. *Nature*. 356:607-9.
- Harrington, L.E., R.D. Hatton, P.R. Mangan, H. Turner, T.L. Murphy, K.M. Murphy, and C.T. Weaver. 2005. Interleukin 17-producing CD4+ effector T cells develop via a lineage distinct from the T helper type 1 and 2 lineages. *Nat Immunol*. 6:1123-32.
- Harris, L.C. 2005. MDM2 splice variants and their therapeutic implications. *Curr Cancer Drug Targets*. 5:21-6.
- Harris, T.J., J.F. Grosso, H.R. Yen, H. Xin, M. Kortylewski, E. Albesiano, E.L. Hipkiss, D. Getnet, M.V. Goldberg, C.H. Maris, F. Housseau, H. Yu, D.M. Pardoll, and C.G. Drake. 2007. Cutting edge: An in vivo requirement for STAT3 signaling in TH17 development and TH17-dependent autoimmunity. *J Immunol*. 179:4313-7.
- Hudson, B.P., M.A. Martinez-Yamout, H.J. Dyson, and P.E. Wright. 2004. Recognition of the mRNA AU-rich element by the zinc finger domain of TIS11d. *Nat Struct Mol Biol*. 11:257-64.
- Hutloff, A., K. Buchner, K. Reiter, H.J. Baelde, M. Odendahl, A. Jacobi, T. Dorner, and R.A. Kroczeck. 2004. Involvement of inducible costimulator in the exaggerated memory B cell and plasma cell generation in systemic lupus erythematosus. *Arthritis Rheum*. 50:3211-20.
- Hutloff, A., A.M. Dittrich, K.C. Beier, B. Eljaschewitsch, R. Kraft, I. Anagnostopoulos, and R.A. Kroczeck. 1999. ICOS is an inducible T-cell co-stimulator structurally and functionally related to CD28. *Nature*. 397:263-6.
- Ivanov, II, B.S. McKenzie, L. Zhou, C.E. Tadokoro, A. Lepelley, J.J. Lafaille, D.J. Cua, and D.R. Littman. 2006. The orphan nuclear receptor ROR γ directs the differentiation program of proinflammatory IL-17+ T helper cells. *Cell*. 126:1121-33.
- Iwai, H., M. Abe, S. Hirose, F. Tsushima, K. Tezuka, H. Akiba, H. Yagita, K. Okumura, H. Kohsaka, N. Miyasaka, and M. Azuma. 2003. Involvement of inducible costimulator-B7 homologous protein costimulatory pathway in murine lupus nephritis. *J Immunol*. 171:2848-54.
- Iwai, H., Y. Kozono, S. Hirose, H. Akiba, H. Yagita, K. Okumura, H. Kohsaka, N. Miyasaka, and M.

- Azuma. 2002. Amelioration of collagen-induced arthritis by blockade of inducible costimulator-B7 homologous protein costimulation. *J Immunol.* 169:4332-9.
- Jackson, R.J., and N. Standart. 2007. How do microRNAs regulate gene expression? *Sci STKE.* 2007:re1.
- Janevay, C.A., P. Travers, M. Walport, and M.J. Shlomchik. 2004. Immunobiology : the immune system in health and disease, 6th edn. New York, Garland Science Publishing.
- Ji, H., A. Pettit, K. Ohmura, A. Ortiz-Lopez, V. Duchatelle, C. Degott, E. Gravallesse, D. Mathis, and C. Benoist. 2002. Critical roles for interleukin 1 and tumor necrosis factor alpha in antibody-induced arthritis. *J Exp Med.* 196:77-85.
- Kaplan, M.H., U. Schindler, S.T. Smiley, and M.J. Grusby. 1996. Stat6 is required for mediating responses to IL-4 and for development of Th2 cells. *Immunity.* 4:313-9.
- Kashanchi, F., and J.N. Brady. 2005. Transcriptional and post-transcriptional gene regulation of HTLV-1. *Oncogene.* 24:5938-51.
- Kassiotis, G., and G. Kollias. 2001. TNF and receptors in organ-specific autoimmune disease: multi-layered functioning mirrored in animal models. *J Clin Invest.* 107:1507-8.
- Kawamoto, M., M. Harigai, M. Hara, Y. Kawaguchi, K. Tezuka, M. Tanaka, T. Sugiura, Y. Katsumata, C. Fukasawa, H. Ichida, S. Higami, and N. Kamatani. 2006. Expression and function of inducible co-stimulator in patients with systemic lupus erythematosus: possible involvement in excessive interferon-gamma and anti-double-stranded DNA antibody production. *Arthritis Res Ther.* 8:R62.
- Kedersha, N., and P. Anderson. 2002. Stress granules: sites of mRNA triage that regulate mRNA stability and translatability. *Biochem Soc Trans.* 30:963-9.
- Khabar, K.S. 2005. The AU-rich transcriptome: more than interferons and cytokines, and its role in disease. *J Interferon Cytokine Res.* 25:1-10.
- Kim, C.H., L.S. Rott, I. Clark-Lewis, D.J. Campbell, L. Wu, and E.C. Butcher. 2001. Subspecialization of CXCR5+ T cells: B helper activity is focused in a germinal center-localized subset of CXCR5+ T cells. *J Exp Med.* 193:1373-81.
- Kloosterman, W.P., and R.H. Plasterk. 2006. The diverse functions of microRNAs in animal development and disease. *Dev Cell.* 11:441-50.
- Klug, A. 1999. Zinc finger peptides for the regulation of gene expression. *J Mol Biol.* 293:215-8.
- Koken, M.H., A. Saib, and H. de The. 1995. A C4HC3 zinc finger motif. *C R Acad Sci III.* 318:733-9.
- Korn, T., E. Bettelli, W. Gao, A. Awasthi, A. Jager, T.B. Strom, M. Oukka, and V.K. Kuchroo. 2007. IL-21 initiates an alternative pathway to induce proinflammatory T(H)17 cells. *Nature.* 448:484-7.
- Lafferty, K.J., L. Andrus, and S.J. Prowse. 1980. Role of lymphokine and antigen in the control of specific T cell responses. *Immunol Rev.* 51:279-314.
- Langrish, C.L., Y. Chen, W.M. Blumenschein, J. Mattson, B. Basham, J.D. Sedgwick, T. McClanahan, R.A. Kastelein, and D.J. Cua. 2005. IL-23 drives a pathogenic T cell population that induces autoimmune inflammation. *J Exp Med.* 201:233-40.
- Laroia, G., B. Sarkar, and R.J. Schneider. 2002. Ubiquitin-dependent mechanism regulates rapid turnover of AU-rich cytokine mRNAs. *Proc Natl Acad Sci U S A.* 99:1842-6.
- Lee, R., R. Feinbaum, and V. Ambros. 2004. A short history of a short RNA. *Cell.* 116:S89-92, 1 p following S96.
- Li, W., B. Gao, S.M. Lee, K. Bennett, and D. Fang. 2007. RLE-1, an E3 ubiquitin ligase, regulates *C. elegans* aging by catalyzing DAF-16 polyubiquitination. *Dev Cell.* 12:235-46.
- Lim, H.W., P. Hillsamer, and C.H. Kim. 2004. Regulatory T cells can migrate to follicles upon T cell activation and suppress GC-Th cells and GC-Th cell-driven B cell responses. *J Clin Invest.* 114:1640-9.
- Ling, V., P.W. Wu, H.F. Finnerty, K.M. Bean, V. Spaulding, L.A. Fouser, J.P. Leonard, S.E. Hunter, R. Zollner, J.L. Thomas, J.S. Miyashiro, K.A. Jacobs, and M. Collins. 2000. Cutting edge: identification of GL50, a novel B7-like protein that functionally binds to ICOS receptor. *J Immunol.* 164:1653-7.
- Liu, Y.J., D.E. Joshua, G.T. Williams, C.A. Smith, J. Gordon, and I.C. MacLennan. 1989. Mechanism of antigen-driven selection in germinal centres. *Nature.* 342:929-31.
- Locksley, R.M., N. Killeen, and M.J. Lenardo. 2001. The TNF and TNF receptor superfamilies: integrating mammalian biology. *Cell.* 104:487-501.
- Mak, T.W., A. Shahinian, S.K. Yoshinaga, A. Wakeham, L.M. Boucher, M. Pintiie, G. Duncan, B.U. Gajewska, M. Gronski, U. Eriksson, B. Odermatt, A. Ho, D. Bouchard, J.S. Whorisky, M. Jordana, P.S. Ohashi, T. Pawson, F. Bladt, and A. Tafuri. 2003. Costimulation through the inducible costimulator ligand is essential for both T helper and B cell functions in T cell-dependent B cell responses. *Nat Immunol.* 4:765-72.
- Mandik-Nayak, L., and P.M. Allen. 2005. Initiation of an autoimmune response: insights from a transgenic model of rheumatoid arthritis. *Immunol Res.* 32:5-13.
- Matzinger, P. 1994. Tolerance, danger, and the extended family. *Annu Rev Immunol.* 12:991-1045.
- McAdam, A.J., R.J. Greenwald, M.A. Levin, T. Chernova, N. Malenkovich, V. Ling, G.J. Freeman, and A.H. Sharpe. 2001. ICOS is critical for CD40-mediated antibody class switching. *Nature.*

- Monticelli, S., K.M. Ansel, C. Xiao, N.D. Socci, A.M. Krichevsky, T.H. Thai, N. Rajewsky, D.S. Marks, C. Sander, K. Rajewsky, A. Rao, and K.S. Kosik. 2005. MicroRNA profiling of the murine hematopoietic system. *Genome Biol.* 6:R71.
- Mosmann, T.R., and R.L. Coffman. 1989. TH1 and TH2 cells: different patterns of lymphokine secretion lead to different functional properties. *Annu Rev Immunol.* 7:145-73.
- Mosmann, T.R., and S. Sad. 1996. The expanding universe of T-cell subsets: Th1, Th2 and more. *Immunol Today.* 17:138-46.
- Nabavi, N., G.J. Freeman, A. Gault, D. Godfrey, L.M. Nadler, and L.H. Glimcher. 1992. Signalling through the MHC class II cytoplasmic domain is required for antigen presentation and induces B7 expression. *In Nature.* Vol. 360. 266-8.
- Nash, P.T., and T.H. Florin. 2005. Tumour necrosis factor inhibitors. *Med J Aust.* 183:205-8.
- Nathan, C. 2002. Points of control in inflammation. *Nature.* 420:846-52.
- Nurieva, R., X.O. Yang, G. Martinez, Y. Zhang, A.D. Panopoulos, L. Ma, K. Schluns, Q. Tian, S.S. Watowich, A.M. Jetten, and C. Dong. 2007. Essential autocrine regulation by IL-21 in the generation of inflammatory T cells. *Nature.* 448:480-3.
- Okamoto, T., S. Saito, H. Yamanaka, T. Tomatsu, N. Kamatani, H. Ogiuchi, T. Uchiyama, and J. Yagi. 2003. Expression and function of the co-stimulator H4/ICOS on activated T cells of patients with rheumatoid arthritis. *J Rheumatol.* 30:1157-63.
- Park, H., Z. Li, X.O. Yang, S.H. Chang, R. Nurieva, Y.H. Wang, Y. Wang, L. Hood, Z. Zhu, Q. Tian, and C. Dong. 2005. A distinct lineage of CD4 T cells regulates tissue inflammation by producing interleukin 17. *Nat Immunol.* 6:1133-41.
- Pesole, G., S. Liuni, G. Grillo, F. Licciulli, F. Mignone, C. Gissi, and C. Saccone. 2002. UTRdb and UTRsite: specialized databases of sequences and functional elements of 5' and 3' untranslated regions of eukaryotic mRNAs. Update 2002. *Nucleic Acids Res.* 30:335-40.
- Pfeffer, K. 2003. Biological functions of tumor necrosis factor cytokines and their receptors. *Cytokine Growth Factor Rev.* 14:185-91.
- Rottman, J.B., T. Smith, J.R. Tonra, K. Ganley, T. Bloom, R. Silva, B. Pierce, J.C. Gutierrez-Ramos, E. Ozkaynak, and A.J. Coyle. 2001. The costimulatory molecule ICOS plays an important role in the immunopathogenesis of EAE. *Nat Immunol.* 2:605-11.
- Schaerli, P., K. Willmann, A.B. Lang, M. Lipp, P. Loetscher, and B. Moser. 2000. CXC chemokine receptor 5 expression defines follicular homing T cells with B cell helper function. *J Exp Med.* 192:1553-62.
- Sharpe, A.H., and G.J. Freeman. 2002. The B7-CD28 superfamily. *Nat Rev Immunol.* 2:116-26.
- Sher, A., and C. Reis e Sousa. 1998. Ignition of the type 1 response to intracellular infection by dendritic cell-derived interleukin-12. *Eur Cytokine Netw.* 9:65-8.
- Sigalas, I., A.H. Calvert, J.J. Anderson, D.E. Neal, and J. Lunec. 1996. Alternatively spliced mdm2 transcripts with loss of p53 binding domain sequences: transforming ability and frequent detection in human cancer. *Nat Med.* 2:912-7.
- Suh, W.K., A. Tafuri, N.N. Berg-Brown, A. Shahinian, S. Plyte, G.S. Duncan, H. Okada, A. Wakeham, B. Odermatt, P.S. Ohashi, and T.W. Mak. 2004. The inducible costimulator plays the major costimulatory role in humoral immune responses in the absence of CD28. *In J Immunol.* Vol. 172. 5917-23.
- Szabo, S.J., S.T. Kim, G.L. Costa, X. Zhang, C.G. Fathman, and L.H. Glimcher. 2000. A novel transcription factor, T-bet, directs Th1 lineage commitment. *Cell.* 100:655-69.
- Tafuri, A., A. Shahinian, F. Bladt, S.K. Yoshinaga, M. Jordana, A. Wakeham, L.M. Boucher, D. Bouchard, V.S. Chan, G. Duncan, B. Odermatt, A. Ho, A. Itie, T. Horan, J.S. Whoriskey, T. Pawson, J.M. Penninger, P.S. Ohashi, and T.W. Mak. 2001. ICOS is essential for effective T-helper-cell responses. *In Nature.* Vol. 409. 105-9.
- Tan, A.H., S.C. Wong, and K.P. Lam. 2006. Regulation of mouse inducible costimulator (ICOS) expression by Fyn-NFATc2 and ERK signaling in T cells. *J Biol Chem.* 281:28666-78.
- Taylor, G.A., E. Carballo, D.M. Lee, W.S. Lai, M.J. Thompson, D.D. Patel, D.I. Schenkman, G.S. Gilkeson, H.E. Broxmeyer, B.F. Haynes, and P.J. Blakeshear. 1996. A pathogenetic role for TNF alpha in the syndrome of cachexia, arthritis, and autoimmunity resulting from tristetraprolin (TTP) deficiency. *Immunity.* 4:445-54.
- Vinuesa, C.G., M.C. Cook, C. Angelucci, V. Athanasopoulos, L. Rui, K.M. Hill, D. Yu, H. Domasch, B. Whittle, T. Lambe, I.S. Roberts, R.R. Copley, J.I. Bell, R.J. Cornall, and C.C. Goodnow. 2005a. A RING-type ubiquitin ligase family member required to repress follicular helper T cells and autoimmunity. *Vol.435.452-8.*
- Vinuesa, C.G., and C.C. Goodnow. 2004. Illuminating autoimmune regulators through controlled variation of the mouse genome sequence. *Immunity.* 20:669-79.
- Vinuesa, C.G., S.G. Tangye, B. Moser, and C.R. Mackay. 2005b. Follicular B helper T cells in antibody responses and autoimmunity. *In Nat Rev Immunol.* Vol. 5. 853-65.

- Warnatz, K., L. Bossaller, U. Salzer, A. Skrabl-Baumgartner, W. Schwinger, M. van der Burg, J.J. van Dongen, M. Orłowska-Volk, R. Knoth, A. Durandy, R. Draeger, M. Schlesier, H.H. Peter, and B. Grimbacher. 2006. Human ICOS deficiency abrogates the germinal center reaction and provides a monogenic model for common variable immunodeficiency. *Blood*. 107:3045-52.
- Weaver, C.T., L.E. Harrington, P.R. Mangan, M. Gavrieli, and K.M. Murphy. 2006. Th17: an effector CD4 T cell lineage with regulatory T cell ties. *Immunity*. 24:677-88.
- Weaver, C.T., R.D. Hatton, P.R. Mangan, and L.E. Harrington. 2007. IL-17 family cytokines and the expanding diversity of effector T cell lineages. *Annu Rev Immunol*. 25:821-52.
- Wienholds, E., and R.H. Plasterk. 2005. MicroRNA function in animal development. *FEBS Lett*. 579:5911-22.
- Winkler, T.H., H. Fehr, and J.R. Kalden. 1992. Analysis of immunoglobulin variable region genes from human IgG anti-DNA hybridomas. *Eur J Immunol*. 22:1719-28.
- Wong, S.C., E. Oh, C.H. Ng, and K.P. Lam. 2003. Impaired germinal center formation and recall T-cell-dependent immune responses in mice lacking the costimulatory ligand B7-H2. *Blood*. 102:1381-8.
- Yang, J.H., J. Zhang, Q. Cai, D.B. Zhao, J. Wang, P.E. Guo, L. Liu, X.H. Han, and Q. Shen. 2005. Expression and function of inducible costimulator on peripheral blood T cells in patients with systemic lupus erythematosus. *Rheumatology (Oxford)*. 44:1245-54.
- Yang, X.O., A.D. Panopoulos, R. Nurieva, S.H. Chang, D. Wang, S.S. Watowich, and C. Dong. 2007. STAT3 regulates cytokine-mediated generation of inflammatory helper T cells. *J Biol Chem*. 282(13):9358-63
- Yoshinaga, S.K., J.S. Whoriskey, S.D. Khare, U. Sarmiento, J. Guo, T. Horan, G. Shih, M. Zhang, M.A. Coccia, T. Kohno, A. Tafuri-Bladt, D. Brankow, P. Campbell, D. Chang, L. Chiu, T. Dai, G. Duncan, G.S. Elliott, A. Hui, S.M. McCabe, S. Scully, A. Shahinian, C.L. Shaklee, G. Van, T.W. Mak, and G. Senaldi. 1999. T-cell co-stimulation through B7RP-1 and ICOS. *Nature*. 402:827-32.
- Yu, D., A.H. Tan, X. Hu, V. Athanasopoulos, N. Simpson, D.G. Silva, A. Hutloff, K.M. Giles, P.J. Leedman, K.P. Lam, C.C. Goodnow, and C.G. Vinuesa. 2007. Roquin represses autoimmunity by limiting inducible T-cell co-stimulator messenger RNA. *Nature*. 450:299-303.
- Zhang, B., Q. Wang, and X. Pan. 2007. MicroRNAs and their regulatory roles in animals and plants. *J Cell Physiol*. 210:279-89.
- Zheng, W., and R.A. Flavell. 1997. The transcription factor GATA-3 is necessary and sufficient for Th2 cytokine gene expression in CD4 T cells. *Cell*. 89:587-96.
- Zhou, L., Ivanov, II, R. Spolski, R. Min, K. Shenderov, T. Egawa, D.E. Levy, W.J. Leonard, and D.R. Littman. 2007. IL-6 programs T(H)-17 cell differentiation by promoting sequential engagement of the IL-21 and IL-23 pathways. *Nat Immunol*. 8:967-74.